Mycoparasitism illuminated by genome sequencing and digital gene expression profiling of Coniothyrium minitans, an important biocontrol fungus of the plant pathogen *Sclerotinia sclerotiorum*

Huizhang Zhao
Huazhong Agriculyural University
Ting Zhou
Huazhong Agricultural University
Jiatao Xie
Huazhong Agricultural University
Jiasen Cheng
Huazhong Agricultural University
Tao Chen
Huazhong Agricultural University
Daohong Jiang
Huazhong Agricultural University
Yanping Fu (yanpingfu@mail.hzau.edu.cn)
Huazhong Agriculture University

Research article

Keywords: Coniothyrium minitans, Sclerotinia sclerotiorum, mycoparasitism, biological control, genome, Different Expression Genes (DEGs)

Posted Date: August 13th, 2019

DOI: https://doi.org/10.21203/rs.2.12750/v1

Abstract

Background

Coniothyrium minitans is a mycoparasite of the notorious plant pathogen Sclerotinia sclerotiorum. To further understand the parasitism of C. minitans, here, we assembled and analyzed its genome by combining transcriptome data.

Results

The genome of C. minitans strain ZS-1 was 39.77 Mb in 350 scaffolds. A total of 11437 predicted genes and proteins were annotated, and 30.8% of blast hits matched proteins encoded by Paraphaeosphaeria sporulosa, a worldwide soil fungus. The transcriptome of strain ZS-1 during the early interaction at 0 h, 4 h and 12 h with its host was analyzed. The detected expressed genes were involved in response to host defenses, including cell wall-degrading enzymes, transporters, secretory proteins and secondary metabolites. The fungal cell wall-degrading enzymes belonged to the GH16, GH18, and GH72 classes in CAZymes, and some were significantly up-regulated during mycoparasitism. Most of the monocarboxylate transporter genes of the major facilitator superfamily and all the detected ABC transporters, especially the heavy metal transporters, were significantly up-regulated. Approximately 8% of the 11437 proteins in C. minitans were predicted to be secretory proteins, with catalytic activity, hydrolase activity, peptidase activity and serine hydrolase activity enriched in molecular function. Most genes involved in serine hydrolase activity were significantly up-regulated during mycoparasitism.

Conclusion

This assemble genome and genome-wide expression study demonstrate that the mycoparasitism process of C. minitans is complex and a series of genes or proteins would be deployed by C. minitans to invade successfully the host. Our study provides insights into the mechanisms of the mycoparasitism between C. minitans and S. sclerotiorum and clues to excavate active secondary metabolites from C. minitans.

Background

Coniothyrium minitans, a sclerotial mycoparasite, lives on the sclerotia of *Sclerotinia sclerotiorum* and its relatives in soil and was first isolated and identified in 1947 by Campbell [1]. It is distributed worldwide in America, Europe, Australia, Africa and Asia [2–4], and its remarkable biocontrol ability has attracted great attention. *C. minitans* shares similar conditions (20°C) with its host *S. sclerotiorum* [1, 4–6]. *C. minitans* has a narrow host range, and most of its reported hosts are fungi in the genus *Sclerotinia* [5]. It can parasitize the sclerotia and hypha of *Sclerotinia* spp. and produce antifungal substances that inhibit host growth [5, 7–13]. *C. minitans* can successfully control crop diseases caused by *S. sclerotiorum* in the field [14–16]. *C. minitans* destroyed the sclerotia, blocked the germination of apothecia by approximately 90% and reduced disease incidence in a bean crop by 50% [5, 17]. As the main effective constituent in

commercial biological control agents, *C. minitans* was first registered in Germany and was used to control the diseases caused by *S. sclerotiorum* and *S. minor* in Europe, America, Oceania and Asia. In China, *C. minitans* agents were also registered to control stem rot of rapeseed caused by *S. sclerotiorum* in 2018.

Mycoparasitism is an important mechanism by which *C. minitans* acts against *S. sclerotiorum. C. minitans* can penetrate both the hyphae and sclerotia of *S. sclerotiorum* [8, 18, 19]. No appressorium-like structures are formed during this mycoparasitism [10]. Mechanical pressure and enzymatic hydrolysis are the two main invasion methods for *C. minitans* to parasitize *S. sclerotiorum* [9, 19–21]. To date, several mycoparasitism-related genes have been identified and verified in *C. minitans.* The fermentation broth of *C. minitans* showed activity of β–1,3-glucan and chitinase and could decompose the cell and cell wall *in vitro* of hyphae and the sclerotia parenchyma cells of *S. sclerotiorum* [9, 22]. The *cmg1* encoding β–1,3-glucanases in *C. minitans* was highly up-regulated, and high activity of chitinase was also detected during mycoparasitism of the sclerotia and hyphae of *S. sclerotiorum [*20, 23–26]. The genes encoding the MAP kinase cascade [27, 28], NADPH oxidase [29], oxalate decarboxylase [30], transcription factors [31–33], the peroxisome [34–36], and heat shock factors [37] have been shown to be highly involved in mycoparasitism in *C. minitans.*

C. minitans may synthesize several secondary substances to inhibit the growth of other fungi or bacteria. The antifungal substances (AFS), mainly macrosphelide A, produced by *C. minitans* could inhibit the hyphal growth of *S. sclerotiorum* and control *Sclerotinia* diseases [7, 13, 38–41]. The production of AFS is regulated by the ambient pH, which is extremely affected by the oxalic acid secreted by *S. sclerotiorum. C. minitans* could synthesizeantibacterial substances (ABS) to inhibit the growth of bacteria in *Clavibacter* and *Xanthomonas* [43, 44]. These ABS may break the balance of the microflora on the plant surface and help *C. minitans* colonize [45].

Although *C. minitans* has been developed as a successful biocontrol agent commercially, its mycoparasitism still needs further investigation to enhance biological control efficiency and to uncover novel genes and active secondary substances; thus, we sequenced the whole genome of *C. minitans* and combined the transcriptome data derived from RNA samples from the early stage of interaction with its host, *S. sclerotiorum.* Based on this analysis, the possible mechanism of mycoparasitism, the potential active secondary substances (antifungal or antibacterial substances) and gene resources for resistance breeding against fungal diseases were discussed.

Results

General features of the *C. minitans* genome

The DNA of *C. minitans* strain ZS–1 was sequenced on the Illumina and PacBio platforms at BGI Technological Company. The 500-bp-long and 6-Kbp-long mate-pair libraries were sequenced using the Illumina platform, and the 20-Kbp-long library was sequenced using the PacBio RS II. The genome

sequence was assembled based on the 6-Kbp-long library data with SOAPdenovo2 [46], the gaps were filled and sequences were extended with the 20 Kbp-long library, and the sequence was corrected using the data from a 500-bp-long library. In all, the data provided an average of 80-fold sequence coverage of the genome (Additional file 1: Table S1). The resulting assembly length was 38.72 Mb across 2,575 contigs, and the N50 length was 64,002 bps. The contigs were assembled into 350 scaffolds that were longer than 1 kb with a total length of 39.77 Mb (including gaps between contigs) using SSPACE [47], and the final N50 length was 653,176 bps (Table 1).

Prediction of the coding proteins and function analysis of C. minitans

Based on the analysis using bioinformatics software and RNA-seq, a total of 11,437 protein-coding genes (11,146 longer than 100 amino acids) were predicted, and all the proteins shared an average length of 481 amino acids (Table 1). Proteins were annotated with the Nr database (non-redundant protein sequences database), GO (Gene Ontology), CDD (Conserved Domain Databases), Pfam domains (protein families and domains), InterPro classification, Swiss-Prot (the section of the Universal Protein Knowledgebase, UniProtKB), GO-Slim (the high-level subset of GO), KEGG (Kyoto Encyclopedia of Genes and Genomes), and KOG (Eukaryotic Orthologous Groups) categories database using Blast2GO (version 5.1) and NCBI-blast program. Hits with an e-value cutoff of 1e−10 and matches of coverage ≥ 0.4 were accepted. On the whole, of all the coding proteins, 10884, 7393, 3193, 7910, 9784, 5888, 7486, 3757 and 8519 were annotated based on the Nr, GO, CDD, Pfam, InterPro, Swiss-Prot, GO-Slim, KEGG and KOG databases, respectively (Additional file 2: Figure S1).

A total of 10884 (94.97%) of the predicted proteins matched the local Nr database (updated on 20180717) with an e-value cutoff of 1e−10, and 32364 blast hits were returned with no more than 3 hits mapped for each protein. The distributions of blast hits in the Nr annotation were determined, and the similarity distribution indicated that 61.11% of all predicted genes of *C. minitans* had over 80% similarity to proteins of other fungal species (Fig. 1a). A total of 30.8% of the protein blast hits mapped to protein sequences from *Paraphaeosphaeria sporulosa* AP3s5-JAC2a, which is saprophytic on wood and has biocontrol ability by nutrition competition and niche occupation [48, 49]; 11.98% of the blast hits mapped to proteins from *Periconia macrospinosa,* a “dark septate endophytic” fungus [50], and 11.51% of the hits matched the proteins of *Corynespora cassiicola,* an endophyte, saprobe or necrotrophic plant pathogen [51]; 5.00% of the blast hits were identified as proteins of *Clohesyomyces aquaticus,* a saprotrophic fungus originally isolated from submerged wood [52]; 4.53% of the blast hits were similar to sequences of *Pyrenochaeta* sp. DS3sAY3a, which plays a role in the bioremediation of metal polluted environments due to the oxidation of manganese (Mn) compounds [48]; 4.26% of the blast hits matched proteins of *Alternaria alternata,* a worldwide plant pathogen known to perform lignocellulose degradation and Mn(II) oxidation [48]; an additional 185 species also matched 5 or more blast hits (Fig. 1b and Additional file 3: Table S2).

Carbohydrate-active enzymes (CAZymes) in *C. minitans*

The complement of each predicted family was conserved in the analyzed fungal genomes from the same order or with similar nutrition type. The CAZyme families predicted in *C. minitans,* along with other fungal genomes from Pleosporales, were classed into a group cluster using principal component analysis (PCA), and the fungi from Hypocreales, Helotiales and Erysiphales were also classified into corresponding groups (Fig. 2a). *Magnaporthe grisea, Fusarium graminearum* and *Aspergillus nidulans* from different orders were grouped into a cluster. Not considering the number of carbohydrate-binding modules (CBMs), *C. minitans* encodes 434 catalytic protein modules in CAZymes, which is moderate compared with the other 39 tested species in our analysis (Additional file 4: Table S3). The number of modules was lower than those in the two phylogenetically nearest fungi, *P. sporulosa* (556) and *Karstenula rhodostoma* (507) and higher than the average level (380) of the three species in *Trichoderma* and two species in *Sclerotinia.* GO analysis showed that the CAZyme protein-coding genes were annotated with functions of catalytic activity (GO: 0003824), carbohydrate binding of (GO: 0030246), transferase activity (GO: 0016757 and GO: 0016758), hydrolase activity (GO: 0016787) ($p \leq 0.05$), cell wall biosynthesis (GO: 0071554) ($p \leq 0.05$) and metabolic process (GO: 0008152) ($p \leq 0.05$) (Additional file 5: Table S4).

The cell wall-degrading enzymes were divided into 2 classes, the plant cell wall-degrading enzymes (PCWDEs) and the fungal cell wall-degrading enzymes (FCWDEs), based on the active domains annotated in the CAZy database. *C. minitans* encodes 118 PCWDEs distributed in 26 families of CAZymes, which is less than its phylogenetically related fungus *P. sporulosa* (170 PCWDEs in the same 25 families) and more than *Trichoderma* spp. (average of 55 in 22 families), *Sclerotinia* spp. (78 in 21 families),and *Botrytis* spp. (101 in 22 families). Ten glycoside hydrolases and 5 polysaccharide lyases were specifically present in *C. minitans,* while 13 and 46 unique orthologous groups were present in *Trichoderma* spp*.* and plant fungal pathogens, respectively. A total of 54 unique orthologous groups (including 58 proteins of *C. minitans)* were shared by *C. minitans* and the other pathogenic fungi analyzed. One orthologous group protein encoding endo–1,4-beta-xylanase (in the GH43 family) was identified in only *C. minitans* and *Trichoderma* spp., while 13 specific orthologous groups were commonly present in *Trichoderma* spp. and the other pathogens (Fig. 2b). These results suggest that *C. minitans* also has the potential to break down the complex composition of plant cell walls.

C. minitans encodes 64 FCWDEs belonging to 14 GH families in CAZymes. *C. minitans* has fewer FCWDEs than *Trichoderma atroviride, Trichoderma harzianum* and *Trichoderma virens,* which have 89, 97 and 97 FCWDEs, respectively. However, pathogenic fungi also have FCWDE families, and their numbers of FCWDEs are similar to those of *C. minitans.* Comparing the FCWDE families of *C. minitans* with those of the selected pathogenic fungi (7 fungi) and *Trichoderma* spp. (3 species), most orthologous groups of *C. minitans* were shared with either *Trichoderma* spp*.* or pathogenic fungi, while 4 unique orthologous groups (4 proteins) were found only in *C. minitans.* These 4 orthologous groups encode glycoside hydrolase family 16 protein (GH16), concanavalin A-like lectin/glucanase (GH16), GPI-anchored cell wall beta–1,3-endoglucanase (GH17) and glycoside hydrolase (GH20). Interestingly, there are 3 orthologous groups shared by *C. minitans* and *Trichoderma* spp. while not existing in the pathogenic fungi tested (Fig. 2c). These 3 orthologous groups encode 4 proteins, one for 2 hexosaminidase (GH20), and the others encode glycoside hydrolase (GH25) and putative exo-beta–1,3-glucanase (GH55), respectively.

Interestingly, *C. minitans* and pathogenic fungi share 47 orthologous groups of FCWDEs (57 proteins) (Fig. 2c).

To investigate the potential CAZyme functions of *C. minitans* during the early stage of interaction with *S. sclerotiorum,* the expression of FCWDEs was examined. The results showed that out of 64 FCWDEs, 45 encoding genes were expressed, and 17 genes were significantly regulated at 4 hpi (hour post inoculation) and 12 hpi; most GH families encoding genes were up-regulated (Fig. 3), while only one GH18 gene (CMZSB_08720), which was distributed in all the fungi tested, was significantly down-regulated. However, the expression of the 4 unique FCWDEs and 3 *Trichoderma*-shared FCWDEs was not significantly altered. Interestingly, PCWDE expression in *C. minitans* was also significantly changed (Additional file 6: Figure S2). These results suggest that cell wall-degrading enzymes may play important roles during the early interaction of *C. minitans* and its host.

MFS and ABC transporters in *C. minitans*

The ATP-binding Cassette (ABC) primary transporter superfamily and the Major Facilitator Superfamily (MFS) are the most ubiquitous transporters in fungi and other organisms [53]. Based on the transporter classification databases (TCDB), the transporters of the MFS superfamily and ABC superfamily were identified in *C. minitans* and 11 other fungal genomes.

A total of 284 predicted MFS transporters of 25 classes were identified in the genome of *C. minitans*. These proteins include Sugar Porter (SP), Drug: H+ Antiporter–1 (12 Spanner) (DHA1), Anion: Cation Symporter (ACS) and Drug: H+ Antiporter–2 (14 Spanner) (DHA2) were the most abundant MFS families in all the detected genomes, including the plant pathogens *Sclerotinia* spp., *B. cinerea, Parastagonospora nodorum* and *Pyrenophora tritici-repentis,* and the biocontrol fungi *Trichoderma* spp. Ten orthologous MFS transporters (10 proteins) were present in *C. minitans* and *Trichoderma* spp. but not in plant pathogenic fungi (Pa). In addition, 32 orthologous transporters (32 proteins) were unique to *C. minitans,* including 5 sugar porters, 4 monocarboxylate transporters (MCT), 9 Anion: Cation symporters, 7 Drug: H+ antiporter–1 (DHA–1), 4 Drug: H+ antiporter–2 (DHA–2) and 3 N-acetylglucosamine transporters (NAG-T) (Fig. 4a and Additional file 7: Table S5).

A total of 185 MFS transporter genes were detected during mycoparasitism at 4 hpi and 12 hpi, and 71 MFS transporters showed significant changes in expression (Fig. 4b). Among the 71 genes, 69 were up-regulated with a siderophore-iron transporter (SIT) gene (*CMZSB_02788),,* and a Fucose: H+ Symporter (FHS) gene (*CMZSB_00290)* was down-regulated. These results indicate that MFS transporters play an important role in the early stage of mycoparasitism. Nine of the 15 MCT protein-encoding genes in *C. minitans* were detected as expressed during the early stages of mycoparasitism. Among these 9 genes, 4 were significantly up-regulated, and one was down-regulated. The results suggest the involvement of MCT in the biocontrol event.

Fifty-one ABC transporters in 13 subfamilies were predicted in *C. minitans,* which is similar to those in *P. sporulosa (*52), *S. sclerotiorum* (49) and *T. atroviride* (51), while the numbers are 44, 47 and 43 in *S. borealis, P. nodorum* and *P. tritici-repentis,* respectively. The numbers of ABC transporters in *B. cinerea* B05.10, *B. cinerea* BcDW1, *T. virens* and *T. harzianum* were 65, 56, 66 and 64, respectively (Additional file 8: Table S6). There were no orthologous ABC transporters identified between *C. minitans* and *Trichoderma* spp., while 23 transporters were present in all the fungi detected (Fig. 5a). This suggests that *C. minitans, Trichoderma* spp. and the plant pathogenic fungi analyzed share a similar transporter distribution of the ABC superfamily, or the function of ABC transporters is conserved in different fungi. *C. minitans* has 7 HMTs (heavy metal transporters), which is almost twice as many as the other 11 fungi analyzed. Group 2983 (TC# 3.A.1.210.1), group 494 (TC# 3.A.1.210.2) and group 242 (TC# 3.A.1.210.2) were present in all fungi analyzed, while *CMZSB_03503 (*TC# 3.A.1.210.2) of Group 12899, *CMZSB_09545* (TC# 3.A.1.210.2) and *CMZSB_11035* (TC# 3.A.1.210.7) were specific to *C. minitans.*

Thirty-six of the 51 ABC transporter genes predicted were up-regulated during the early stages of mycoparasitism in *C. minitans,* and 23 were significantly altered (Fig. 5b). Five of the 7 HMT coding genes, including *CMZSB_03503* (orthologous groups 12899) and *CMZSB_09545* (specific to *C. minitans),*, were significantly up-regulated at the primary stage of infection (Fig. 5b), and all 7 genes were mapped to the iron-binding (GO: 0005506) molecular function based on GO.

Secretory proteins enriched in the mycoparasitism process in *C. minitans*

A total of 908 secretory proteins were predicted in *C. minitans,* accounting for 8.29% of the total proteins. The proportion of secretory proteins was 5.50% in *Sclerotinia* spp., 6.52% in *Botrytis* spp., 6.66% in *Trichoderma* spp., and 9.36% in *P. sporulosa.* Taking no account of CAZymes, the 695 predicted secretory proteins were classified into 675 orthologous groups, and 45 were unique to *C. minitans* without orthologs in *Trichoderma* spp. or the 7 selected plant pathogens in our analysis. In addition, 307, 499 and 1041 specific orthologs were predicted in *C. minitans, Trichoderma* spp. and the pathogenic fungi, respectively. Twenty-four orthologous groups were specific to *C. minitans* and *Trichoderma* spp. and absent in pathogenic fungi. The 45 unique proteins in *C. minitans* were annotated, and the results showed a PR–1-like protein (CMZSB_08830), an Acyl-CoA N-acyltransferase (CMZSB_04745), an amino acid transporter (CMZSB_05748), a protein with the DUF605 multi-domain (CMZSB_00858), and a FAD/NAD(P)-binding domain-containing protein (CMZSB_06166); 40 proteins were unknown proteins or hypothetical proteins with no specific functions reported.

A total of 526 secretory protein-coding genes were detected during the early mycoparasitism stages of *C. minitans,* and 132 DEGs were predicted via CAZymes. The DEGs were enriched in catalytic activity (GO: 0003824), hydrolase activity (GO: 0016787), peptidase activity (GO: 0008233) and serine hydrolase activity (GO: 0017171) in molecular function ($p \leq 0.01$); 51 DEGs were enriched in extracellular region (GO: 0005576) in cellular component ($p \leq 0.01$). Almost all the related genes involved in the serine

peptidase activity GO term were up-regulated significantly in the early stages of mycoparasitism in *C. minitans,* with the exception of CMZSB_02437, a gene encoding an Asp-domain-containing protein (Fig. 6).

Eighty effector-like proteins were identified in *C. minitans* strain ZS–1, and for 50 of them, expression of their encoding genes was detected as related to mycoparasitism. Four effector-like encoding genes (*CMZSB_03902, CMZSB_06513, CMZSB_08537* and *CMZSB_09504)* from the *C. minitans* genome were transformed into the host fungus (*S. sclerotiorum* strain 1980) with the help of *Agrobacterium.* All of them had an influence on the transformed colonies of *S. sclerotiorum,* including partial inhibition of the hyphal growth rates of a number of transformants (data not shown). More analysis should be conducted on these four effector-like genes to elucidate their functions during mycoparasitism.

PKS- and NRPS-encoding genes and their expression in *C. minitans*

The *C. minitans* genome encodes 7 non-ribosomal peptide synthases (NRPS) clusters, 6 type I polyketide synthases (PKS) (t1PKS) clusters, 1 type III PKS (t3PKS) cluster and 1 hybrid t1PKS-NRPS gene cluster. Six NRPS clusters were detected with 6 different structures in *C. minitans* ZS–1. An NRPS-like cluster with additional sites of nicotinamide adenine dinucleotide (NAD) and another cluster with a thioesterase domain (TD) were also identified (Fig. 7).

During the early stages of mycoparasitism in *C. minitans,* 53 DEGs were identified among the genes detected in the PKS and NRPS biosynthesis gene clusters. Of these, 31 were up-regulated at 4 hpi, while 40 were up-regulated and 7 were down-regulated at 12 hpi. At the later mycoparasitism stage (12 h versus 4 h), 13 genes were up-regulated, and 8 were down-regulated (Fig. 7). Most core biosynthetic genes of NRPS involved in mycoparasitism were up-regulated, with the NRPS–3-related core gene CMZSB_06212 and the NRPS–6-related gene *CMZSB_10567* down-regulated significantly. The expression of all the core biosynthetic genes of t1PKS, t3PKS and hybrid t1PKS-NRPS were significantly induced when in contact with *S. sclerotiorum.* The t1PKS encoding gene *CmPKS1* (*CMZSB_04445)* was proven to be associated with the mycoparasitism of *C. minitans* [54].

Nine genes in five clusters related to gliotoxin were annotated in *C. minitans:* GliA (gliotoxin A) (CMZSB_02816), 2 GliI (gliotoxin I) (CMZSB_02903 and CMZSB_03980), 2 GliK (gliotoxin K) (CMZSB_03977 and CMZSB_08616), 2 GliC (gliotoxin C) (CMZSB_03976 and CMZSB_03979), 1 GliT (gliotoxin T) (CMZSB_03988) and 1 GliP (gliotoxin P) (CMZSB_03975) involved in gliotoxin biosynthesis. The expression of these genes could not be detected at 4 hpi, and only 2 were expressed at 12 hpi. One or more of these genes may play important roles in the mycoparasitism of *C. minitans* on *S. sclerotiorum.* Three of the gliotoxin-related genes were mapped to the function of oxidoreductase activity (GO: 0016491), and three steps related to oxidation in gliotoxin biosynthesis were predicted from the only known intermediate compounds cyclo-L-phenylalanyl-L-serine (Gardiner and Howlett, 2005). The

CMZSB_02816 was annotated into MFS gliotoxin efflux transporter and was similar to the protein GliA reported from *Aspergillus fumigatus,* which plays a significant role in tolerance to gliotoxin and protection from extracellular gliotoxin [55].

Discussion

In this study, the genome of *C. minitans* was sequenced, assembled and annotated, and the potential mechanism of parasitism was analyzed based on the RNA-seq data. The size of the genome of *C. minitans* is approximately 39.77 Mb, which is moderate among ascomycetes. *C. minitans* has a large number of genes encoding enzymes for both plant and fungal cell wall degradation; it also has many genes for MFS and ABC transporters, PKS and NRPS; a high proportion of genes coding for secretory proteins were also predicted.

Plant and fungal cell wall degrading enzymes in *C. minitans*

C. minitans has 434 putative catalytic protein modules in CAZymes, and this number is moderate compared with the other 39 fungal species in our study; many of these proteins were predicted to be enzymes for degrading either plant cell walls or fungal cell walls. The number of genes coding for PCWDEs is not smaller than those of plant necrotrophic pathogenic fungi, such as *M. oryzae, B. cinerea* and its host, *S. sclerotiorum,* and it is significantly larger than those of biotrophic fungal pathogens. Compared to pathogenic fungi, *C. minitans* has 17 unique PCWDEs (distributed in 15 orthologous proteins). These genes may enable *C. minitans* to live on dead plants. Interestingly, in this study, we found that the expression of many PCWDE genes was highly induced at the early stage of *C. minitans* contact with *S. sclerotiorum,* suggesting that these PCWDEs may also play some role in parasitizing *S. sclerotiorum;* further experiments are needed to confirm this hypothesis.

FCWDEs may play essential roles in fungal development [56–58]; thus, no fungi without FCWDEs could survive in nature. As a mycoparasite, *C. minitans* might reasonably have a powerful fungal cell wall-degrading enzyme system to attack *S. sclerotiorum.* However, the number of FCWDE genes in *C. minitans* is not significantly different from that in plant pathogenic fungi; furthermore, *C. minitans* shared 47 orthologous FCWDEs with the pathogenic fungi tested. Interestingly, the mycoparasitic *Trichoderma* spp. have many more FCWDEs than *C. minitans,* and the GH18 family is considered to play an important role during mycoparasitization [59–62]. Only three orthologs in GH18were shared by *C. minitans* and *Trichoderma* spp., but they were not detected during the early stage of interaction between *C. minitans* and *S. sclerotiorum.* The chitinase gene (*CMZSB_00640)* and β–1,3-endo-glucanase (*CMZS_02526)* of *C. minitans* are usually used as two marker genes for mycoparasitism [63], while their orthologs can also be identified in pathogenic fungi. Furthermore, these two genes and *CMZSB_02023* (encoding chitinase) were also up-regulated significantly (log2 ratio > 2.5, FDR ≤ 0.001) at conidiationdata not shown). This evidence suggests that the FCWDEs of *C. minitans* may play a role not only in parasitizing *S. sclerotiorum* but also in shaping the cell walls of *C. minitans,*asinplant pathogens [64].

Secondary metabolites and their functions in *C. minitans*

Fungi are known to produce a large number of secondary metabolites, and genes for secondary metabolites are often distributed in clusters on genomes. Many biocontrol agents can produce antagonistic secondary metabolites to suppress the growth of pathogens or to occupy advantageous niches [65–67]. Early experiments found that *C. minitans* could produce both antifungal substances and antibacterial substances [13, 43], among which macrosphelide A has antimicrobial activity against some ascomycetes, such as *Sclerotinia* spp., basidiomycetes, oomycetes and Gram-positive bacteria [41, 68]. Macrosphelide A, benzenediol and 5-aminopentanoate were the three most accumulated compounds when *C. minitans* was co-cultured with *S. sclerotiorum* for 2 days [40].

PKS) and NRPS are the main synthases of polyketides and peptides. As in *S. sclerotiorum, B. cinerea, P. nodorum* and mycoparasitic *Trichoderma* spp., *C. minitans* contains gene clusters related to secondary metabolism, including 7 NRPS clusters, 6 t1PKS clusters, 1 t3PKS cluster, and 1 hybrid t1PKS-NRPS gene cluster. The number of related genes was counted within each cluster, and no significant difference was found with the comparison of all the tested fungal genomes among genes related to the t1PKS clusters. Previously, we identified a type I PKS gene (*CmPKS1)* and found that disruption of *CmPKS1* led to an absence of melanin but could not significantly affect the mycoparasitism of *S. sclerotiorum* [54]. Disruption of *CmMR1,* a transcription factor gene, blocked the production of melanin but could not affect the mycoparasitism of *C. minitans* [31].

Gliotoxin is a secondary metabolite produced by many fungi. It can suppress immunity, promote apoptosis of mammalian cells [69] and inhibit the growth of microorganisms by disrupting NAPDH oxidase activity [70]. The non-ribosomal peptide synthetase GliP in *A. fumigatus* catalyzes the first biosynthetic step in the synthesis of gliotoxin and was reported as the determinant of host-specific virulence [71]. When *gliP* was disrupted, *T. virens* lost the ability to produce gliotoxin and parasitize *S. sclerotiorum* [72]; *T. virens* and *T. harzianum* have 6 [69, 73] and 9 NRPS-encoding genes, respectively, but non-mycoparasitic *Trichoderma reesei* has 9 genes in the biosynthetic cluster. Although gliotoxin has not yet been identified, a NRPS cluster with 9 genes related to gliotoxin synthesis was predicted on Scaffold 12 and annotated in *C. minitans.* The homologous gene clusterof gliotoxin biosynthesis in *C. minitans* displays a similarity of 47% with that of *T. reesei* and much lower with that of the biocontrol *Trichoderma* species. We speculate that *C. minitans* encodes a type of gliotoxin biosynthetic gene cluster different from those in biocontrol *Trichoderma* spp. but similar to that in *T. reesei.* Two of the annotated gliotoxin-related genes were up-regulated at 12 hpi with *S. sclerotiorum.* This evidence suggests that gliotoxin or gliotoxin-like substances may be synthesized and contribute to the parasitism of *C. minitans.*

MFS and ABC transporters in *C. minitans*

The MFS transporter superfamily and ABC transporter superfamily are the most ubiquitous transporters in fungi and other organisms [53]. MFS transporters and ABC transporters play very important roles in

resistance against drug and plant toxic components for pathogens and are also very important for beneficial microorganisms [74–77]. The expression of MFS transporters and ABC transporters was induced in *C. minitans* during interaction with *S. sclerotiorum,* suggesting that these two classes of transporters may play important roles in the mycoparasitism process.

Siderophores are responsible for the storage of iron and the protection of cells from oxidative stress [78, 79]. In *T. virens,* deletion of TvTex10, an intracellular siderophore biosynthesis-related gene, increased the fungal growth rate and sensitivity to oxidative stress and simultaneously decreased conidia and gliotoxin production [80]. Fifty-four ABC transporters in 14 subfamilies were predicted in *C. minitans.* Interestingly, there are 7 heavy metal transporters (HMTs) in *C. minitans,*while only 3–4 HMTs were found in the other fungi tested; 6 of them have putative iron-binding functions and were expressed during the early interaction between *C. minitans* and *S. sclerotiorum. CmSIT1,* a siderophore iron transporter gene (*CMZSB_03548)* annotated in Scaffold 10, was expressed when contacting *S. sclerotiorum* but not when growing on PDA [39]. The results demonstrate that SITs and related HMTs are important for the acquisition of iron by mycoparasites in a competitive environment and are involved in mycoparasitism.

Effector-like proteins in *C. minitans*

Typical effectors are small cysteine-rich secretory proteins (usually less than 150 aa) and are released by pathogens into host cells to disrupt the host's resistance system. Cerato-platanin proteins are effectors for many pathogenic fungi [81] and were also identified in *Trichoderma* spp.,which could induce plant defense against pathogens [82]. SM1, an elicitor of induced systemic resistance (ISR), was identified as an effector-like protein involved in the colonization of maize roots by *T. virens* [83]. In *Trichoderma* spp., 233 effector-like proteins have been annotated, and a Class II hydrophobin family gene *tvhyiil,* could help *T. virens* colonize plant roots and participate in antagonistic activity against *Rhizoctonia solani* [84]. In this study, 80 genes encoding effector-like proteins were identified in *C. minitans,*and 50 of them were expressed during the early stage of interaction between *C. minitans* and *S. sclerotiorum.* We further found that some of these effector-like protein genes could induce a hypersensitive reaction when transiently expressed in the leaves of *Nicotiana benthamiana,* and four other effector-like protein genes led to a decrease in hyphal growth when expressed in *S. sclerotiorum,* suggesting that some of these effector-like proteins may potentially function in plants, and some may function in the parasitism of *C. minitans.* It may not be surprising that *Trichoderma* spp. release effector-like proteins into plant cells, because they can live endophytically in plant roots. However, *C. minitans* is a soil-borne fungus and has not been found to live in plants. Considering that *C. minitans* can parasitize only fungi in the genus *Sclerotinia,* we hypothesize that some effector-like proteins of *C. minitans* may specifically function in recognition of *Sclerotinia* spp. Further investigation is necessary to confirm the functions of effector-like proteins in the interaction between the host fungus and mycoparasite.

Complicated mechanism of mycoparasitism in *C. minitans*

Previously, a model for the interaction between *C. minitans* and *S. sclerotiorum* was established. *C. minitans* senses the oxalic acid produced by *S. sclerotiorum* or the low pH caused by oxalic acid and produces antifungal substances to inhibit the growth of *S. sclerotiorum* and degrade the oxalic acid with oxalate decarboxylase; after the ambient pH rises, *C. minitans* secretes fungal cell wall degrading enzymes and enters the parasitic life stage [30, 32]. However, in this interaction system, although *C. minitans* could produce antifungal substances to weaken *S. sclerotiorum* and destroy the cell wall of *S. sclerotiorum* using FCWDEs, counteraction by *S. sclerotiorum* should be considered. As shown in this study, many genes for MFS transporters, ABC transporters, effector-like proteins and secondary metabolites were significantly up-regulated during the early stage of interaction, suggesting that these substances play essential roles in parasitism of *S. sclerotiorum.* ABC transporters, especially HMTs, may be used by *C. minitans* to compete with *S. sclerotiorum* for heavy metal elements such as iron; MFS transporters may have two functions, to release antifungal substances and in efflux of toxic compounds produced by *S. sclerotiorum.* There is a high possibility that the effector-like proteins enter the hyphae of *S. sclerotiorum* and specifically inhibit the counteraction system of *S. sclerotiorum.* Once it subdues *S. sclerotiorum, C. minitans* carries on a parasitic life in its host (Fig. 8).

Conclusions

Given that our study assembled the genome of the important mycoparasite of the plant pathogen *S. sclerotiorum* firstly, and analyzed the orthologous proteins between the biocontrol fungi and other two group fungi (biocontrol group of *Trichoderma* and plant pathogens group of 7 selected pathogens in our study) to develop the possible mycoparasitism mechanism. Combining with the RNA-seq of mycoparasitism process, the genes expression related mycoparasitism was detected to elucidate the process of mycoparasitism in *C. minitans* with its host *S. sclerotiorum.* Our analysis sheds light on the mycoparasitism of *C. minitans* and provides clues to excavate active secondary metabolites from *C. minitans.*

Tables

Table 1 The statistics assembly of the *C. minitans* ZS-1 genome sequence features

Genome feature	*Coniothyrium minitans* ZS-1
Size (bp, draft)	39,772,940
Number of Scaffolds	350
Scaffold N50length (bp)*	653,176
G+C content	51.70%
Scaffold minimum length(bp)	1,007
Scaffold maximum length/bp	1,862,540
Total gene size (bp)	22,430,464
Protein-coding genes	11,437
Average coded protein length (AA)	481
Predicted proteins with signal peptide	1171

* Scaffold N50, scaffold length at which 50% of total bases in the assembly are in scaffolds of that length or greater.

Materials And Methods

Strain and growth conditions

C. minitans strain ZS−1, originally isolated from a single conidium of *C. minitans* in China, was used for genome sequencing. *S. sclerotiorum* 1980 was used for the “virulence test”. All fungi were grown on PDA (BD, Sparks, MD, USA) plates at 20 °C.

Nucleic acid preparation and sequencing

Genomic DNA of *C. minitans* strain ZS−1 was extracted following [85] with minor modification. Briefly, 2% sodium lauroyl sarcosine (SLS) fungal DNA extraction reagent containing 2% w/v SLS, 100 mM pH 8.0 Tris-HCl, 20 mM EDTA and 100 mM NaCl was used to extract genomic DNA from 4 days cultured hyphal of *C. minitans* strain ZS−1.

- minitans strain ZS−1 was sequenced by Illumina HiSeq sequencing (Illumina, CA, USA) and PacBio RS II sequencing (Pacific Biosciences, CA, USA) platforms at Beijing Genomics Institute (BGI, Shenzhen, Guangdong, China). A total of three libraries (one sequenced by our lab in 2008) were used for genome analysis: a 500 bp paired-end shotgun library, one 6 Kbp mate-pair library for

illumine HiSeq and one 20 Kbp library for PacBio RS II. The genomic DNA was purified using magnetic beads method at BGI for preparing DNA library.

In additional, 15 RNA-seq libraries corresponding to the growth and development stages of *C. minitans* ZS–1 were used to helping with prediction of transcripts. Conidia were collected from PDA slants and washed with sterilized water twice to remove culture residues. A total of 400 μL of spore suspension at 10^6/mL was evenly spread on the PDA plate, which was covered with cellophane. To provide evidence for the genes predicted in *C. minitans* ZS–1, samples of *C. minitans* at different stages, namely, conidial germination (24 h), hyphal growth early (36 h), hyphal growth late (48 h), pycnidia formation (72 h) and mature conidia (0 h), were collected, quickly frozen in liquid nitrogen and stored at –80°C for RNA extraction, with three repeats for each sample. All 15 RNA samples were used to make the sequencing libraries and analyzed via an Illumina HiSeq 2500 at a read length of PE150 (150 bp paired-end [PE] reads).

To extract the RNA samples of *C. minitans* interacting with *S. sclerotiorum,* conidia of strain ZS–1 were shaken at 20°C in PDB at 100 rpm for 36 h, washed with sterilized water 3 times and re-suspended in water at 10^6 /mL. The conidial suspension was coated on a 24-hour-old colony of *S. sclerotiorum.* Three mixed mycelial samples were collected at 0 hpi (immediately after coating), 4 hpi (coculture for 4 h), and 12 hpi (co-culture for 12 h), and RNA was extracted. RNA was generated using RNA reagent (NewBio Industry, Tianjin, China) following the instructions. The mixed RNA samples were sequenced via an Illumina HiSeq 2000 at 49 bps of single-end read at BGI.

Genome assembly

Genome assemblies were performed using the SOAPdenovo2 (SOAPdenovo2, RRID: SCR_014986) [46] genome assembler with the 6 Kbp mate-pair library data. The best preassembly of a longer N50 contig size and a lower number of the contigs was assembled as the initial assembly (Version1.0). The GapCloser v1.12 (GapCloser, RRID: SCR 015026) was used to fill gaps into Version1.0; then, the contigs were linked to assemble genome scaffolds using the software SSPACE (SSPACE, RRID: SCR_005056) with the PacBio library data [47, 86]. The scaffolds of the initial assembly were against to the NCBI NT database (08/17/2016) (ftp://ftp.ncbi.nlm.nih.gov/blast/db/) testing for removing the contamination by bacteria or other organisms. With removing the length under 1 Kbp of the initial assembly scaffolds, the other kept scaffolds were the final assembled genome sequences of *C. minitans* ZS–1.

Genome annotation

Gene predictions on the masked genome were performed using both transcript mapping-based and *ab initio* methods. *Transcript mapping-based methods:* Transcripts were generated by first mapping the RNA-seq reads to the assembled genome using Hisat2 (Hisat2, RRID: SCR_015530) [87, 88], and SAMtools (Samtools, RRID: SCR_002105) [89] was used to convert the sam files to bam files. A set of transcripts

was generated by Cufflinks (Cufflinks, RRID: SCR_014597) with the mapping data [90, 91]. Unmapped reads from the 15 RNA libraries were *de novo* assembled using Trinity (Trinity, RRID: SCR_013048) [92, 93]. Then, the Cufflinks transcripts and Trinity-assembled transcripts were combined to get an initial gene models (GeneModel v1.1). The second gene models (GeneModel v1.2) was performed based on the RNA-seq using program to assemble spliced alignments (PASA) (PASA, RRID: SCR_014656) [94]. *Ab initio methods:* GeneMark (GeneMark, RRID: SCR_011930) [95, 96] was used to generate an set of gene models (GeneModel v2.1). The BAM mapping file generated by TopHat v2.1.1 (TopHat, RRID: SCR_013035) [87] was used to generate an intron/exon hint file. The file was used to predict another gene models (GeneModel v2.2) using Augustus v3.2.3 (Augustus, RRID: SCR_008417). Gene model evidence from RNA-seq based (GeneModel v1.1 and GeneModel v1.2) and *ab inito* methods (GeneModel v2.1 and GeneModel v2.2) were imported into the EVidenceModeler package (EVidenceModeler, RRID: SCR_014659) [97, 98] for consensus gene model predictions. Higher weight was given to the RNA-seq alignment predictions than to the ab initio predictions. The RNA-seq data were mapped to the repeat-masked genome and used to update the set of gene models using PASA. Genes with 150 nt or more were considered in the subsequent analysis. After removing duplicated sequences using Blast2GO (Blast2GO, RRID: SCR_005828), artificial intelligence error correction of the final predicted genes was performed using WebApollo (WebApollo: A Web-Based Sequence Annotation Editor for Community Annotation, RRID: SCR_005321) [99] with evidence of gene prediction.

Orthologous protein analysis

We used the OrthoMCL DB v2.0.9 (OrthoMCL DB: Ortholog Groups of Protein Sequences, RRID: SCR_007839) [100] to identify orthologs of protein clusters between *C. minitans* and 38 other ascomycete genomes, including the host fungi *S. sclerotiorum* 1980 UF–70 and *S. borealis* F–4128, 3 nonhost plant pathogens (*B. cinerea* BcDW1, B05.10 and T4); 3 “dark septate entophytic” fungi (DSE) (*Paraphaeosphaeria sporulosa* AP3s5-JAC2a, *Periconia macrospinosa* DSE2036, and *Stagonospora* sp. SRC1lsM3a) [48]; 3 biocontrol fungi in the *Trichoderma* genus (*Trichoderma atroviride, Trichoderma harzianum* and *Trichoderma virens);*; 3 hemi-biotrophic plant pathogens (*Fusarium graminearum* PH–1, *Magnaporthe oryzae* 70–15, and *Colletotrichum higginsianum* IMI 349063); 3 biotrophic plant pathogens (*Erysiphe necator, Erysiphe pulchra* Cflorida, and *Blumeria graminis* f. sp. *hordei* DH14); 10 necrotrophic plant pathogens (*Phaeosphaeria nodorum* N15, *Pyrenophora tritici-repentis* Pt–1C-BFP, *Corynespora cassiicola* Philippines, *Ascochyta rabiei* ArDII, *Leptosphaeria maculans* JN3, *Alternaria alternata* SRC1lrK2f, *Bimuria novae-zelandiae* CBS 107.79, *Bipolaris maydis* ATCC 48331, *Bipolaris oryzae* ATCC 44560 and *Bipolaris sorokiniana* ND90Pr); 7 saprotrophic fungi (*Neurospora crassa* OR74A, *Karstenula rhodostoma, Didymocrea sadasivanii, Byssothecium circinans, Massarina eburnean, Lentithecium fluviatile,* and *Trematosphaeria pertusa),*, and 3 model fungi (*Saccharomyces cerevisiae* S288C, *Schizosaccharomyces pombe* 972h, and *Aspergillus nidulans* FGSC A4). All the proteins of the detected species were downloaded from NCBI or JGI.

Orthologous protein groups were picked from the above results of the Cm group (*C. minitans* ZS−1, also considering *P. sporulosa* AP3s5-JAC2a); Tr group (*T. atroviride, T. harzianum* and *T. virens);*, Pa group (including the host fungi *S. sclerotiorum* 1980 UF−70 and *S. borealis* F−4128; 3 nonhost fungi of plant pathogens (*B. cinerea* BcDW1, B05.10 and T4); and 2 necrosis plant pathogenic fungi (*P. nodorum* N15 and *P. tritici-repentis* Pt−1C-BFP).

Functional annotation

Nr annotation, Gene Ontology (GO) and InterPro identification were performed using Blast2GO [101]. Encoding protein sequences of *C. minitans* were annotated into databases of UniProtKB/Swiss-Prot database (RRID: SCR 004426) [102, 103], KOG (KOG: Phylogenetic Clusters of Orthologous Groups Ranking, RRID: SCR_008223) [104], CDD (updated 03/28/2017) (CDD: Conserved Domain Database, RRID: SCR_002077) [105] and Pfam domains (Pfam 31, 16712 families) (Pfam, RRID: SCR_004726) [106] with using NCBI blastp (blastp, RRID: SCR_001010) with an e-value cutoff of 1e−5, respectively. KEGG analyses were performed using the KAAS online webserver [107].

Identification of carbohydrate-active enzymes *(CAZymes)*

We took into account all presented CAZyme classes: Glycoside Hydrolases (GH), Glycoside Transferase (GT), Polysaccharide Lyases (PL), Carbohydrate Esterases (CE), Auxiliary redox enzymes (AA) and Carbohydrate-Binding Modules (CBM). FCWEs and PCWEs were classified based on the annotations in the CAZy database. Genomes of *C. minitans* and 38 other fungi were screened for CAZymes in this study. NCBI blastp and dbCAN server (dbCAN, RRID: SCR_013208) [108, 109] were conducted against the sequence libraries and profiles in the CAZy database (http://www.cazy.org/) (CAZy-Carbohydrate Active Enzyme, RRID: SCR_012909). All positive matched hits no less than 0.5 were examined manually for final predictions.

MFS and ABC transporter proteins of *C. minitans*

All the predicted proteins in *C. minitans* were blasted against the transporter classification database (TCDB) (TCDB, RRID: SCR_004490) [110, 111] with diamond blastp (Diamond, RRID: SCR_009457) [112] with a high scoring pair (HSP) with an expectation value (e-value) cutoff of $1e^{-5}$. The query coverage was set at ≥ 50%, and the identity level was ≥ 20%. The blastp results were scanned under the TMHMM server v.2.0 (TMHMM server, RRID: SCR_014935) [113] with ≥ 10 transmembrane helices (TMHs). The proteins were classified into 1345 families based on phylogenetic, sequence, structural and functional analyses in TCDB using the Transporter Classification (TC) system.

Identification of secondary metabolite biosynthesis gene clusters

Identification of secondary metabolite biosynthesis gene clusters was carried out using the genome assemblies and annotation files of *C. minitans* and 11 other genomes: *P. sporulosa, P. tritici-repentis, P. nodorum, S. sclerotiorum, S. borealis, B. cinerea* B05.10, *B. cinerea* BcT4, *B. cinerea* BcDW1, *T. atroviride, T. harzianum* and *T. virens.* The algorithm of antiSMASH fungal (version 4.0) with the default parameters was used to predict the secondary metabolite-encoding gene clusters [114, 115]. The gene clusters of PKS and NRPS were investigated based on the prediction results.

Secretome prediction

Protein sequences with extracellular secretary signals were predicted using SignalP 4.1 (SignalP, RRID: SCR_015644) [116, 117] with the default settings for eukaryotic organisms. Proteins were considered to be secreted if the signal peptide probability was greater than or equal to 0.90 and a cleavage site was within the first approximately 25 amino acids. These predictions were further refined using TargetP v1.1 with a non-plant program and default cutoff parameters [118, 119], and candidate secreted proteins predicted to target the mitochondria were discarded. Subsequently, these candidate secreted proteins were checked for transmembrane domains using TMHMM v.2.0 [113, 120]. Finally, the candidate secreted proteins were compared by WoLF PSORT (WoLF PSORT, RRID: SCR_002472) [121] with the weighted k-nearest neighbor classifier no less than 15. Putative small secreted proteins (SSPs), which were also considered effectors, were predicted as no more than 300 amino acids and cysteine content with no less than 4%.

Analysis of differentially expressed genes (DEGs) at different interaction time points

The raw RNA data from the three libraries were sequenced via Illumina HiSeq 2000. Adaptors, reads with more than 10% unknown bases and low-quality reads (quality value ≤ 5 of a read) were removed from the raw reads to obtain the clean reads. The clean reads were mapped tothe *C. minitans* genome using SOAP aligner/soap2 [122]. Mismatches of no more than 2 bases were allowed in the alignment. The gene expression level was calculated using the RPKM method (reads per kb per million reads) [123].

A method described in “The significance of digital gene expression profiles” [124] was used to screen the DEGs. We used FDR (False Discovery Rate) ≤ 0.001 and the absolute value of $\log_2$ ratio ≥ 1.5 as the threshold to judge the significance of gene expression differences.

Three groups of RPKM-based gene expression data were obtained from the 3 mixed RNA-seq libraries based on the genomes of *S. sclerotiorum* and *C. minitans.* CmSs0h, CmSs4h and CmSs12h represented the gene expression of *C. minitans* at 0 h, 4 h and 12 h mycoparasitism stages with *S. sclerotiorum,* respectively. Gene expression data of *C. minitans* in SsCm0h, SsCm4h and SsCm12h with clean reads ≥ 10 in one of the time points during the mycoparasitism stage of *C. minitans* with *S. sclerotiorum* were retained. Based on the gene RPKM value data, a series of comparison groups was conducted to analyze

the mycoparasitism genes at the primary interaction stage. We examined the DEGs at different interaction times, and three comparisons were conducted: CmSs0–4, gene expression of *C. minitans* in interaction 4 h versus 0 h; CmSs0–12, 4 h versus 0 h; CmSs4–12, 12 h versus 4 h.

Abbreviations

Blast: Basic Local Alignment Search Tool; PacBio: Pacific Bioscience; bp, base pairs; NCBI: National Center for Biotechnology Information; RNA-seq: RNA sequencing; Kbp, Thousands of base pairs; Mb, Millions of base pairs; Gb, Giga of base pairs; JGI, doe joint genome institute. Nr database: non-redundant protein sequences database; GO: Gene Ontology; CDD: conserved domain databases; Pfam domains: protein families and domains; Swiss-Prot: the section of the UniProtKB (Universal Protein Knowledgebase); GO-Slim: the high-level subset of GO; KEGG: Kyoto Encyclopedia of Genes and Genomes; KOG: Eukaryotic Orthologous Groups; PCA: principal component analysis; CBMs: carbohydrate-binding modules; CAZymes: Carbohydrate-active enzymes; PCWDEs: plant cell wall-degrading enzymes; FCWDEs: fungal cell wall-degrading enzymes; MFS: Major Facilitator Superfamily; TCDB: the transporter classification databases; PKS: Polyketide synthases; NRPS: non-ribosomal peptide synthases; GliP: gliotoxin P; GliA: gliotoxin A; hpi: hour post inoculation (co-culture hours of *C. minitans* with *S. sclerotiorum)*..

Declarations

Ethics approval and consent to participate

Not applicable.

Not applicable.

Availability of data and materials

This Whole Genome Shotgun project has been deposited at DDBJ/ENA/GenBank under the accession VFEO00000000. The version described in this paper is version VFEO01000000. The genome of *C. minitans* ZS–1 assembly and raw data are available via the NCBI Sequence Read Archive (SRA) with BioProject: PRJNA548470, BioSample: SAMN12034817, SRA: SRR9290694-SRR9290696. The interaction mapped RNA-seq data files of 0 hpi, 4 hpi and 12 hpi were uploaded with bam files in SRA: SRR9301107-SRR9301109, respectively, into BioSample: SAMN12046022 under BioProject: PRJNA548660.

Competing interests

The authors declare no competing interests.

Funding

This research was supported by the National Key R&D Program of China (2017YFD0200400), the National Natural Science Foundation of China (Grant 31572048), and the earmarked fund for China Agriculture Research System (CARS–13).

Authors' contributions

- F. and D. J. designed and managed the project. H. Z. and T. Z. collected materials, prepared and purified DNA and RNA samples for the genome sequencing and RNA-seq. H. Z., T. Z., J. X., T. C. and J. C. performed the genome assemblies and genome annotations. H. Z., Y. F. and D. J. wrote the manuscript.

Acknowledgement

We would like to acknowledge the anonymous reviewers for their work on this paper.

Additional Files

Additional file 1: Table S1. Library data showing the sequence coverage of *Coniothyrium minitans* ZS–1.

Additional file 2: Figure S1. Statistical numbers of protein-coding genes in *C. minitans* ZS–1 as predicted by different databases. Nr: Non-redundant database (Nr); Swiss_Prot: UniProtKB/Swiss-Prot; InterPro: InterPro database; GO: Gene Ontology; CDD: NCBI Conserved Domain Database; Pfam: Pfam database; GO-Slim: GO-code Enzyme; KEGG: Kyoto Encyclopedia of Genes and Genomes Pathway Annotation; KOG: Eukaryotic Orthologous Groups Annotation.

Additional file 3: Table S2. Species distribution of the 11437 proteins in *Coniothyrium minitans* ZS–1 based on the Non-redundant (NR) annotation.

Additional file 4: Table S3. Distribution of CAZymes in *Coniothyrium minitans* ZS–1 and other detected genomes in our analyses.

Additional file 5: Table S4. GO enrichment analysis of the identified CAZymes in *Coniothyrium minitans* ZS–1.

Additional file 6: Figure S2. Expression of PCWDEs in the CAZymes detected in mycoparasitism. (A) RPKM values of 3 interaction time points (0 h, 4 h and 12 h) of CAZymes related to degradation of pectin, hemicellulose and cellulose; (B) Gene expression of degrading lignin detected during the early mycoparasitism stages. CmSs0h-RPKM, CmSs0h-RPKM and CmSs0h-RPKM: RPKM values of expression at 0 hpi, 4 hpi and 12 hpi.

Additional file 7: Table S5. Statistics of MFS transporters in *Coniothyrium minitans* ZS–1 and other fungal genomes analyzed in this research.

Additional file 8: Table S6. ABC distribution of detected fungi in the research within *Coniothyrium minitans* ZS–1.

References

1.Campbell WA. A new species of *Coniothyrium* parasitic on sclerotia. Mycologia.1947; 39(2):190–195.

2.Sandyswinsch C, Whipps JM, Gerlagh M, Kruse M. World distribution of the sclerotial mycoparasite *Coniothyrium minitans.* Mycol Res.1993; 97:1175–8.

3.Huang HC. Distribution of *Coniothyrium minitans* in Manitoba sunflower fields. Can J Plant Pathol.1981; 3(4):219–22.

4.Li G, Wang D, Zhang S, Dan H. Characterization of the sclerotial parasite *Coniothyrium minitans.* 1995; 14(2):125–30.

5.Whipps JM, Gerlagh M. Biology of *Coniothyrium minitans* and its potential for use in disease biocontrol. Mycol Res.1992; 96(11):897–907.

6.Trutmann P, Keane PJ, Merriman PR. Reduction of sclerotial inoculum of *Sclerotinia sclerotiorum* with *Coniothyrium minitans.* Soil Biol Biochem.1980; 12(5):461–5.

7.Yang R, Han YC, Li GQ, Jiang DH, Huang HC. Suppression of *Sclerotinia sclerotiorum* by antifungal substances produced by the mycoparasite *Coniothyrium minitans.* Eur J Plant Pathol.2007; 119(4):411–20.

8.Tu JC. Mycoparasitism by *Coniothyrium minitans* on *Sclerotinia sclerotiorum* and its effect on sclerotial germination. J Phytopathol.1984; 109(3):261–8.

9.Huang HC, Kokko EG. Penetration of hyphae of *Sclerotinia sclerotiorum* by *Coniothyrium minitans* without the formation of appressoria. J Phytopathol.1988; 123(2):133–9.

10.Huang HC, Hoes JA. Penetration and Infection of *Sclerotinia Sclerotiorum* by *Coniothyrium minitans.* Can J Bot.1976; 54(5–6):406–10.

11.Turner GJ, Tribe HT. On *Coniothyrium minitans* and its parasitism of sclerotinia species. T Brit Mycol Soc.1976; 66(Feb):97–105.

12.Li GQ, Huang HC, Miao HJ, Erickson RS, Jiang DH, Xiao YN. Biological control of sclerotinia diseases of rapeseed by aerial applications of the mycoparasite *Coniothyrium minitans.* Eur J Plant Pathol.2006; 114(4):345–55.

13.McQuilken MP, Gemmell J, Whipps JM. Some nutritional factors affecting production of biomass and antifungal metabolites of *Coniothyrium minitans.* Biocontrol Sci Techn.2002; 12(4):443–54.

14.Budge SP, Whipps JM. Potential for integrated control of *Sclerotinia sclerotiorum* in glasshouse Lettuce using *Coniothyrium minitans* and reduced fungicide application. Phytopathology.2001; 91(2):221–7.

15.Chitrampalam P, Wu BM, Koike ST, Subbarao KV. Interactions between *Coniothyrium minitans* and *Sclerotinia minor* affect biocontrol efficacy of *C. minitans.* Phytopathology.2011; 101(3):358–66.

16.Elsheshtawi M, Elkhaky MT, Sayed SR, Bahkali AH, Mohammed AA, Gambhir D, Mansour AS, Elgorban AM. Integrated control of white rot disease on beans caused by *Sclerotinia sclerotiorum* using Contans and reduced fungicides application. Saudi J Biol Sci.2017; 24(2):405–9.

17.Gerlagh M, Goossen-van de Geijn HM, Fokkema NJ, Vereijken PF. Long-term biosanitation by application of *Coniothyrium minitans* on *Sclerotinia sclerotiorum* infected crops. Phytopathology.1999; 89(2):141–7.

18.Jones D, Johnson RPC. Ultrastructure of frozen, fractured and etched pycnidiospores of *Coniothyrium minitans.* T Brit Mycol Soc.1970; 55:83–7.

19.Huang HC, Kokko EG. Ultrastructure of hyperparasitism of *Coniothyrium minitans* on sclerotia of *Sclerotinia sclerotiorum.* Can J Bot.1987; 65(12):2483–9.

20.Jones D, Gordon AH, Bacon JS. Co-operative action by endo- and exo-beta-(1 leads to 3)-glucanases from parasitic fungi in the degradation of cell-wall glucans of *Sclerotinia sclerotiorum* (Lib.) de Bary. Biochem J.1974; 140(1):47–55.

21.Phillips AJL, Price K. Structural aspects of the parasitism of sclerotia of *Sclerotinia sclerotiorum* (Lib) Debary by *Coniothyrium minitans* Campb. J Phytopathol.1983; 107(3):193–203.

22.Hu Y, Li G, Yang L. Characterization of factors affecting enzymatic activity of chitinase produced by mycoparasite *Coniothyrium minitans.* Chin J Appl Environ Biol.2010; 2009(2):226–9.

23.Giczey G, Kerenyi Z, Fulop L, Hornok L. Expression of cmg1, an exo-beta–1,3-glucanase gene from *Coniothyrium minitans,* increases during sclerotial parasitism. Appl Environ Microbiol.2001; 67(2):865–71.

24.Ren L, Li G, Han YC, Jiang DH, Huang H-C. Degradation of oxalic acid by *Coniothyrium minitans* and its effects on production and activity of beta–1,3-glucanase of this mycoparasite. Biol Control.2007; 43(1):1–11.

25.Gao J, Wang J, Li X, Ma L. Dynamic changes of cell wall-degrading enzyme and effect during *Coniothyrium minitans* parasiting on *Sclerotinia sclerotiorum.* 2007; 35(11):13–6.

26.Kaur J, Munshi GD, Singhi RS, Koch E. Effect of carbon source on production of lytic enzymes by the sclerotial parasites *Trichoderma atroviride* and *Coniothyrium minitans.* J Phytopathol.2005; 153(5):274–9.

27.Zeng F, Gong X, Hamid MI, Fu Y, Jiatao X, Cheng J, Li G, Jiang D. A fungal cell wall integrity-associated MAP kinase cascade in *Coniothyrium minitans* is required for conidiation and mycoparasitism. Fungal Genet Biol.2012; 49(5):347–57.

28.Wei W. Identifition of conidiation and growth associated genes in *Coniothyrium minitans.* Huazhong Agricultural University, Wuhan, CHINA, 2013.

29.Wei W, Zhu W, Cheng J, Xie J, Jiang D, Li G, Chen W, Fu Y. Nox Complex signal and MAPK cascade pathway are cross-linked and essential for pathogenicity and conidiation of mycoparasite *Coniothyrium minitans.* Sci Rep.2016; 6:24325.

30.Zeng LM, Zhang J, Han YC, Yang L, Wu MD, Jiang DH, Chen W, Li GQ. Degradation of oxalic acid by the mycoparasite *Coniothyrium minitans* plays an important role in interacting with *Sclerotinia sclerotiorum.* Environ Microbiol.2014; 16(8):2591–610.

31.Luo C, Zhao H, Yang X, Qiang C, Cheng J, Xie J, Chen T, Jiang D, Fu Y. Functional analysis of the melanin-associated gene *CmMR1* in *Coniothyrium minitans.* Front Microbiol.2018; 9:2658.

32.Lou Y, Han Y, Yang L, Wu M, Zhang J, Cheng J, Wang M, Jiang D, Chen W, Li G. CmpacC regulates mycoparasitism, oxalate degradation and antifungal activity in the mycoparasitic fungus *Coniothyrium minitans.* Environ Microbiol.2015; 17(11):4711–29.

33.Han Y, Li G, Yang L, Jiang D. Molecular cloning, characterization and expression analysis of a pacC homolog in the mycoparasite *Coniothyrium minitans.* World J Microbiol Biotechnol.2010; 27(2):381–91.

34.Wei W, Zhu W, Cheng J, Xie J, Li B, Jiang D, Li G, Yi X, Fu Y. *CmPEX6,* a gene involved in peroxisome biogenesis, is essential for parasitism and conidiation by the sclerotial parasite *Coniothyrium minitans.* Appl Environ Microbiol.2013; 79(12):3658–66.

35.Guo Y. Cloning and functional analysis of conidiation associated gene CMPEX2 of *Coniothyrium minitans.* Huazhong Agricultural University, Wuhan, CHINA, 2008.

36.Wu S. Partial Cloning Conidiation-Associated Gene of Coniothyrium minitans and Improving its Conidia Production in Shaken Liquid Medium. Huazhong Agricultural University, Wuhan, CHINA, 2006.

37.Hamid MI, Zeng F, Cheng J, Jiang D, Fu Y. Disruption of heat shock factor 1 reduces the formation of conidia and thermotolerance in the mycoparasitic fungus *Coniothyrium minitans.* Fungal Genet Biol.2013; 53:42–9.

38.Yang R, Han Y, Li G, Jiang D, Huang H-C. Effects of ambient pH and nutritional factors on antifungal activity of the mycoparasite *Coniothyrium minitans.* Biol Control.2008; 44(1):116–27.

39.Sun XP, Zhao Y, Jia JC, Xie JT, Cheng JS, Liu HQ, Jiang DH, Fu YP. Uninterrupted Expression of *CmSIT1* in a sclerotial parasite *Coniothyrium minitans* leads to reduced growth and enhanced antifungal ability. Front Microbiol.2017; 8:2208.

40.He Z, Hu X, Fu Y, Jiang D. Metabolic profile of *Coniothyrium minitans* co-cultured with *Sclerotinia sclerotiorum.* 2017; 36(1):35–41.

41.McQuilken MP, Gemmell J, Hill RA, Whipps JM. Production of macrosphelide A by the mycoparasite *Coniothyrium minitans.* FEMS Microbiol Lett.2003; 219(1):27–31.

42.Yin X. Partial cloning antibacterial substances-associated gene of Coniothyrium minitans and studying ecological function of antibacterial substances. Huazhong Agricultural University, Wuhan, CHINA, 2007.

43.Jiang D, Li G, Yi X, Fu Y, Wang D. Studies on the properties of antibacterial substance produced by *Coniothyrium minitans.* Acta Phytopathol Sin.1998; 28(1):29–32.

44.Wang H, Hu X, Jiang D. Separation of the metabolic product of *Coniothyrium minitans* against *Xanthomonas oryzae* pv. oryzae. 2009; 28(2):148–150.

45.Yang L, Miao HJ, Li GQ, Yin LM, Huang HC. Survival of the mycoparasite *Coniothyrium minitans* on flower petals of oilseed rape under field conditions in central China. Biol Control.2007; 40(2):179–86.

46.Luo R, Liu B, Xie Y, Li Z, Huang W, Yuan J, He G, Chen Y, Pan Q, Liu Y *et al.* SOAPdenovo2: an empirically improved memory-efficient short-read de novo assembler. GigaScience.2012; 1(1).

47.Boetzer M, Henkel CV, Jansen HJ, Butler D, Pirovano W. Scaffolding pre-assembled contigs using SSPACE. Bioinformatics.2011; 27(4):578–9.

48.Zeiner CA, Purvine SO, Zink EM, Paša-Tolić L, Chaput DL, Haridas S, Wu S, LaButti K, Grigoriev IV, Henrissat B *et al.* Comparative analysis of secretome profiles of Manganese(II)-oxidizing ascomycete fungi. PLoS One.2016; 11(7):e0157844.

49.Turhan G. Further hyperparasites of Rhizoctonia solarni Kühn as promising candidates for biological control / Weitere Hyperparasiten von Rhizoctonia solani Kühn als aussichtsreiche Kandidaten für eine biologische Bekämpfung. J Plant Dis Protect.1990; 97(2):208–15.

50.Knapp DG, Nemeth JB, Barry K, Hainaut M, Henrissat B, Johnson J, Kuo A, Lim JHP, Lipzen A, Nolan M *et al.* Comparative genomics provides insights into the lifestyle and reveals functional heterogeneity of dark septate endophytic fungi. Sci Rep.2018; 8(1):6321.

51.Lopez D, Ribeiro S, Label P, Fumanal B, Venisse JS, Kohler A, de Oliveira RR, Labutti K, Lipzen A, Lail K *et al.* Genome-wide analysis of *Corynespora cassiicola* leaf fall disease putative effectors. Front Microbiol.2018; 9:276.

52.Zhang H, Hyde KD, McKenzie EHC, Bahkali AH, Zhou D. Sequence data reveals phylogenetic affinities of *Acrocalymma aquatica* sp. nov., *Aquasubmersa mircensis* gen. et sp. nov. and *Clohesyomyces aquaticus* (Freshwater Coelomycetes). Cryptogamie Mycol.2012; 33(3):333–46.

53.Perlin MH, Andrews J, Toh SS. Essential letters in the fungal alphabet: ABC and MFS transporters and their roles in survival and pathogenicity. Adv Genet.2014; 85:201–253.

54.Xiang Y. Cloning and functional analysis of melanins associated gene *CmPKS1* in *Coniothyrium minitans.* Huazhong Agricultural University, Wuhan, CHINA, 2011.

55.Wang DN, Toyotome T, Muraosa Y, Watanabe A, Wuren T, Bunsupa S, Aoyagi K, Yamazaki M, Takino M, Kamei K. GliA in *Aspergillus fumigatus* is required for its tolerance to gliotoxin and affects the amount of extracellular and intracellular gliotoxin. Med Mycol.2014; 52(5):506–18.

56.Donzelli BG, Harman GE. Interaction of ammonium, glucose, and chitin regulates the expression of cell wall-degrading enzymes in *Trichoderma atroviride* strain P1. Appl Environ Microbiol.2001; 67(12):5643–5647.

57.Gruber S, Seidl-Seiboth V. Self versus non-self: fungal cell wall degradation in *Trichoderma.* Microbiology.2012; 158(Pt 1):26–34.

58.Gow NAR, Latge J-P, Munro CA. The fungal cell wall: structure, biosynthesis, and function. Microbiol Spectr.2017; 5(3):1–25.

59.Kubicek CP, Herrera-Estrella A, Seidl-Seiboth V, Martinez DA, Druzhinina IS, Thon M, Zeilinger S, Casas-Flores S, Horwitz BA, Mukherjee PK *et al.* Comparative genome sequence analysis underscores mycoparasitism as the ancestral life style of *Trichoderma.* Genome Biol.2011; 12(4):R40.

60.Seidl V, Huemer B, Seiboth B, Kubicek CP. A complete survey of *Trichoderma* chitinases reveals three distinct subgroups of family 18 chitinases. FEBS J.2005; 272(22):5923–39.

61.Carsolio C, Benhamou N, Haran S, Cortes C, Gutierrez A, Chet I, Herrera-Estrella A. Role of the *Trichoderma harzianum* endochitinase gene, *ech42,* in mycoparasitism. Appl Environ Microbiol.1999; 65(3):929–935.

62.Martinez D, Berka RM, Henrissat B, Saloheimo M, Arvas M, Baker SE, Chapman J, Chertkov O, Coutinho PM, Cullen D *et al.* Genome sequencing and analysis of the biomass-degrading fungus *Trichoderma reesei* (syn. *Hypocrea jecorina)*.. Nat Biotechnol.2008; 26(5):553–60.

63.Yang X, Cui H, Cheng J, Xie J, Jiang D, Hsiang T, Fu Y. A HOPS protein, CmVps39, is required for vacuolar morphology, autophagy, growth, conidiogenesis and mycoparasitic functions of *Coniothyrium minitans.* Environ Microbiol.2016; 18(11):3785–97.

64.Lyu X, Shen C, Fu Y, Xie J, Jiang D, Li G, Cheng J. Comparative genomic and transcriptional analyses of the carbohydrate-active enzymes and secretomes of phytopathogenic fungi reveal their significant roles during infection and development. Sci Rep.2015; 5:15565.

65.Keller NP. Fungal secondary metabolism: regulation, function and drug discovery. Nat Rev Microbiol.2019; 17(3):167–80.

66.Vinale F, Sivasithamparam K, Ghisalberti EL, Marra R, Barbetti MJ, Li H, Woo SL, Lorito M. A novel role for *Trichoderma* secondary metabolites in the interactions with plants. Physiol Mol Plant P.2008; 72(1–3):80–6.

67.Mukherjee PK, Horwitz BA, Kenerley CM. Secondary metabolism in *Trichoderma* - a genomic perspective. Microbiology.2012; 158(Pt 1):35–45.

68.Tomprefa N, McQuilken MP, Hill RA, Whipps JM. Antimicrobial activity of *Coniothyrium minitans* and its macrolide antibiotic macrosphelide A. J Appl Microbiol.2009; 106(6):2048–56.

69.Scharf DH, Brakhage AA, Mukherjee PK. Gliotoxin—bane or boon? Environ Microbiol.2016; 18(4):1096–1109.

70.Tsunawaki S, Yoshida LS, Nishida S, Kobayashi T, Shimoyama T. Fungal metabolite gliotoxin inhibits assembly of the human respiratory burst NADPH oxidase. Infect Immun.2004; 72(6):3373.

71.Spikes S, Xu R, Nguyen CK, Chamilos G, Kontoyiannis DP, Jacobson RH, Ejzykowicz DE, Chiang LY, Filler SG, May GS. Gliotoxin production in *Aspergillus fumigatus* contributes to host-specific differences in virulence. J Infect Dis.2008; 197(3):479–86.

72.Vargas WA, Mukherjee PK, Laughlin D, Wiest A, Moran-Diez ME, Kenerley CM. Role of gliotoxin in the symbiotic and pathogenic interactions of *Trichoderma virens.* Microbiology.2014; 160(Pt 10):2319–30.

73.Atanasova L, Le Crom S, Gruber S, Coulpier F, Seidl-Seiboth V, Kubicek CP, Druzhinina IS. Comparative transcriptomics reveals different strategies of *Trichoderma* mycoparasitism. BMC Genet.2013; 14:121.

74.Woo SL, Scala F, Ruocco M, Lorito M. The molecular biology of the interactions between *Trichoderma* spp., phytopathogenic fungi, and plants. Phytopathology.2006; 96(2):181–5.

75.Ruocco M, Lanzuise S, Vinale F, Marra R, Turra D, Woo SL, Lorito M. Identification of a new biocontrol gene in *Trichoderma atroviride:* the role of an ABC transporter membrane pump in the interaction with different plant-pathogenic fungi. Mol Plant Microbe Interact.2009; 22(3):291–301.

76.Karlsson M, Durling MB, Choi J, Kosawang C, Lackner G, Tzelepis GD, Nygren K, Dubey MK, Kamou N, Levasseur A *et al.* Insights on the evolution of mycoparasitism from the genome of *Clonostachys rosea.* Genome Biol Evol.2015; 7(2):465–80.

77.Dubey MK, Jensen DF, Karlsson M. An ATP-binding cassette pleiotropic drug transporter protein is required for xenobiotic tolerance and antagonism in the fungal biocontrol agent *Clonostachys rosea.* Mol Plant Microbe Interact.2014; 27(7):725–32.

78.Oide S, Krasnoff SB, Gibson DM, Turgeon BG. Intracellular siderophores are essential for ascomycete sexual development in heterothallic *Cochliobolus heterostrophus* and homothallic *Gibberella zeae.* Eukaryot Cell.2007; 6(8):1339–53.

79.Wallner A, Blatzer M, Schrettl M, Sarg B, Lindner H, Haas H. Ferricrocin, a siderophore involved in intra- and transcellular iron distribution in *Aspergillus fumigatus.* Appl Environ Microbiol.2009; 75(12):4194–6.

80.Mukherjee PK, Hurley JF, Taylor JT, Puckhaber L, Lehner S, Druzhinina I, Schumacher R, Kenerley CM. Ferricrocin, the intracellular siderophore of *Trichoderma virens,* is involved in growth, conidiation, gliotoxin biosynthesis and induction of systemic resistance in maize. Biochem Biophys Res Commun.2018; 505(2):606–11.

81.Pazzagli L, Seidl-Seiboth V, Barsottini M, Vargas WA, Scala A, Mukherjee PK. Cerato-platanins: elicitors and effectors. Plant Sci.2014; 228:79–87.

82.Gomes EV, Costa Mdo N, de Paula RG, de Azevedo RR, da Silva FL, Noronha EF, Ulhoa CJ, Monteiro VN, Cardoza RE, Gutierrez S *et al.* The cerato-platanin protein Epl–1 from *Trichoderma harzianum* is involved in mycoparasitism, plant resistance induction and self cell wall protection. Sci Rep.2015; 5:17998.

83.Crutcher FK, Moran-Diez ME, Ding S, Liu J, Horwitz BA, Mukherjee PK, Kenerley CM. A paralog of the proteinaceous elicitor SM1 is involved in colonization of maize roots by *Trichoderma virens.* Fungal Biol.2015; 119(6):476–86.

84.Guzmán-Guzmán P, Alemán-Duarte MI, Delaye L, Herrera-Estrella A, Olmedo-Monfil V. Identification of effector-like proteins in *Trichoderma* spp. and role of a hydrophobin in the plant-fungus interaction and mycoparasitism. BMC Genet.2017; 18(1):16.

85.Cai W, Xu D, Xia L, Xie H, Wei J. A new method for the extraction of fugal genomic DNA. 2014; 152(3):1–5.

86.Boetzer M, Pirovano W. SSPACE-LongRead: scaffolding bacterial draft genomes using long read sequence information. BMC Bioinformatics.2014; 15(1):211.

87.Kim D, Pertea G, Trapnell C, Pimentel H, Kelley R, Salzberg SL. TopHat2: accurate alignment of transcriptomes in the presence of insertions, deletions and gene fusions. Genome Biol.2013; 14(4):R36.

88.Goldstein LD, Cao Y, Pau G, Lawrence M, Wu TD, Seshagiri S, Gentleman R. Prediction and quantification of splice events from RNA-seq data. 2016; 11(5):e0156132.

89.Li H, Handsaker B, Wysoker A, Fennell T, Ruan J, Homer N, Marth G, Abecasis G, Durbin R, Genome Project Data Processing S. The Sequence Alignment/Map format and SAMtools. Bioinformatics.2009; 25(16):2078–9.

90.Ghosh S, Chan C-KK. Analysis of RNA-Seq Data Using TopHat and Cufflinks. In: Edited by Edwards D, editors. Plant Bioinformatics: Methods and Protocols. New York, NY: Springer New York; 2016. p 339–361.

91.Trapnell C, Roberts A, Goff L, Pertea G, Kim D, Kelley DR, Pimentel H, Salzberg SL, Rinn JL, Pachter L. Differential gene and transcript expression analysis of RNA-seq experiments with TopHat and Cufflinks. Nat Protoc.2012; 7(3):562–78.

92.Grabherr MG, Haas BJ, Yassour M, Levin JZ, Thompson DA, Amit I, Adiconis X, Fan L, Raychowdhury R, Zeng Q *et al.* Full-length transcriptome assembly from RNA-seq data without a reference genome. Nat Biotechnol.2011; 29(7):644–52.

93.Haas BJ, Papanicolaou A, Yassour M, Grabherr M, Blood PD, Bowden J, Couger MB, Eccles D, Li B, Lieber M *et al. De novo* transcript sequence reconstruction from RNA-seq using the Trinity platform for reference generation and analysis. Nat Protoc.2013; 8(8):1494–512.

94.Haas BJ, Zeng Q, Pearson MD, Cuomo CA, Wortman JR. Approaches to fungal genome annotation. 2011; 2(3):118–41.

95.Besemer J, Borodovsky M. GeneMark: web software for gene finding in prokaryotes, eukaryotes and viruses. Nucleic Acids Res.2005; 33(Web Server issue):W451–4.

96.Hoff KJ, Lange S, Lomsadze A, Borodovsky M, Stanke M. BRAKER1: Unsupervised RNA-seq-based genome annotation with GeneMark-ET and AUGUSTUS. Bioinformatics.2016; 32(5):767–9.

97.Li Z, Zhang Z, Yan P, Huang S, Fei Z, Lin K. RNA-Seq improves annotation of protein-coding genes in the cucumber genome. BMC Genet.2011; 12:540.

98.Haas BJ, Salzberg SL, Zhu W, Pertea M, Allen JE, Orvis J, White O, Buell CR, Wortman JR. Automated eukaryotic gene structure annotation using EVidenceModeler and the program to assemble spliced alignments. Genome Biol.2008; 9(1):R7.

99.Lee E, Helt GA, Reese JT, Munoz-Torres MC, Childers CP, Buels RM, Stein L, Holmes IH, Elsik CG, Lewis SE. Web Apollo: a web-based genomic annotation editing platform. Genome Biol.2013; 14(8):R93.

100.Fischer S, Brunk BP, Chen F, Gao X, Harb OS, Iodice JB, Shanmugam D, Roos DS, Stoeckert Jr. CJ. Using OrthoMCL to Assign Proteins to OrthoMCL-DB Groups or to Cluster Proteomes Into New Ortholog

Groups. Curr Protoc Bioinformatics.2011; 35(1):6.12.11–19.

101.Conesa A, Gotz S, Garcia-Gomez JM, Terol J, Talon M, Robles M. Blast2GO: a universal tool for annotation, visualization and analysis in functional genomics research. Bioinformatics.2005; 21(18):3674–6.

102.The UniProt C. UniProt: the universal protein knowledgebase. Nucleic Acids Res.2017; 45(D1):D158–69.

103.Chen C, Huang H, Wu CH. Protein bioinformatics databases and resources. In: Edited by Wu CH, Arighi CN, Ross KE, editors. Protein Bioinformatics: From Protein Modifications and Networks to Proteomics. New York, NY: Springer New York; 2017. p 3–39.

104.Galperin MY, Makarova KS, Wolf YI, Koonin EV. Expanded microbial genome coverage and improved protein family annotation in the COG database. Nucleic Acids Res.2015; 43(Database issue):D261–9.

105.Marchler-Bauer A, Bo Y, Han L, He J, Lanczycki CJ, Lu S, Chitsaz F, Derbyshire MK, Geer RC, Gonzales NR *et al.* CDD/SPARCLE: functional classification of proteins via subfamily domain architectures. Nucleic Acids Res.2017; 45(D1):D200–3.

106.Finn RD, Coggill P, Eberhardt RY, Eddy SR, Mistry J, Mitchell AL, Potter SC, Punta M, Qureshi M, Sangrador-Vegas A *et al.* The Pfam protein families database: towards a more sustainable future. Nucleic Acids Res.2016; 44(D1):D279–85.

107.Moriya Y, Itoh M, Okuda S, Yoshizawa AC, Kanehisa M. KAAS: an automatic genome annotation and pathway reconstruction server. Nucleic Acids Res.2007; 35(Web Server issue):W182–5.

108.Zhang H, Huang L, Wu P, Yang Z, Entwistle S, Yohe T, Yin Y, Busk PK, Xu Y. dbCAN2: a meta server for automated carbohydrate-active enzyme annotation. Nucleic Acids Res.2018; 46(W1):W95-W101.

109.Yin Y, Mao X, Yang J, Chen X, Mao F, Xu Y. dbCAN: a web resource for automated carbohydrate-active enzyme annotation. Nucleic Acids Res.2012; 40(Web Server issue):W445–51.

110.Saier MH, Jr., Reddy VS, Tsu BV, Ahmed MS, Li C, Moreno-Hagelsieb G. The Transporter Classification Database (TCDB): recent advances. Nucleic Acids Res.2016; 44(D1):D372-D9.

111.Saier MH, Jr., Tran CV, Barabote RD. TCDB: the Transporter Classification Database for membrane transport protein analyses and information. Nucleic Acids Res.2006; 34(Database issue):D181–6.

112.Buchfink B, Xie C, Huson DH. Fast and sensitive protein alignment using DIAMOND. Nat Methods.2015; 12(1):59–60.

113.Krogh A, Larsson B, von Heijne G, Sonnhammer EL. Predicting transmembrane protein topology with a hidden markov model: application to complete genomes. J Mol Biol.2001; 305(3):567–80.

114.Blin K, Medema MH, Kottmann R, Lee SY, Weber T. The antiSMASH database, a comprehensive database of microbial secondary metabolite biosynthetic gene clusters. Nucleic Acids Res.2017; 45(D1):D555–9.

115.Medema MH, Blin K, Cimermancic P, de Jager V, Zakrzewski P, Fischbach MA, Weber T, Takano E, Breitling R. antiSMASH: rapid identification, annotation and analysis of secondary metabolite biosynthesis gene clusters in bacterial and fungal genome sequences. Nucleic Acids Res.2011; 39(Web Server issue):W339–46.

116.Nielsen H. Predicting Secretory Proteins with SignalP. In: Edited by Kihara D, editors. Protein Function Prediction: Methods and Protocols. New York, NY: Springer New York; 2017. p 59–73.

117.Petersen TN, Brunak S, von Heijne G, Nielsen H. SignalP 4.0: discriminating signal peptides from transmembrane regions. Nat Methods.2011; 8:785.

118.Emanuelsson O, Brunak S, von Heijne G, Nielsen H. Locating proteins in the cell using TargetP, SignalP and related tools. Nat Protoc.2007; 2(4):953–71.

119.Emanuelsson O, Nielsen H, Brunak S, von Heijne G. Predicting subcellular localization of proteins based on their N-terminal amino acid sequence. J Mol Biol.2000; 300(4):1005–16.

120.Sonnhammer ELL, Heijne Gv, Krogh A. A Hidden Markov Model for Predicting Transmembrane Helices in Protein Sequences. In: Proceedings of the 6th International Conference on Intelligent Systems for Molecular Biology. 663187: AAAI Press 1998: 175–82.

121.Horton P, Park KJ, Obayashi T, Fujita N, Harada H, Adams-Collier CJ, Nakai K. WoLF PSORT: protein localization predictor. Nucleic Acids Res.2007; 35(Web Server issue):W585–7.

122.Li R, Yu C, Li Y, Lam TW, Yiu SM, Kristiansen K, Wang J. SOAP2: an improved ultrafast tool for short read alignment. Bioinformatics.2009; 25(15):1966–7.

123.Mortazavi A, Williams BA, McCue K, Schaeffer L, Wold B. Mapping and quantifying mammalian transcriptomes by RNA-Seq. Nat Methods.2008; 5(7):621.

124.Audic Sp, Claverie J-M. The Significance of Digital Gene Expression Profiles. Genome Res.1997; 7(10):989–95.

Figures

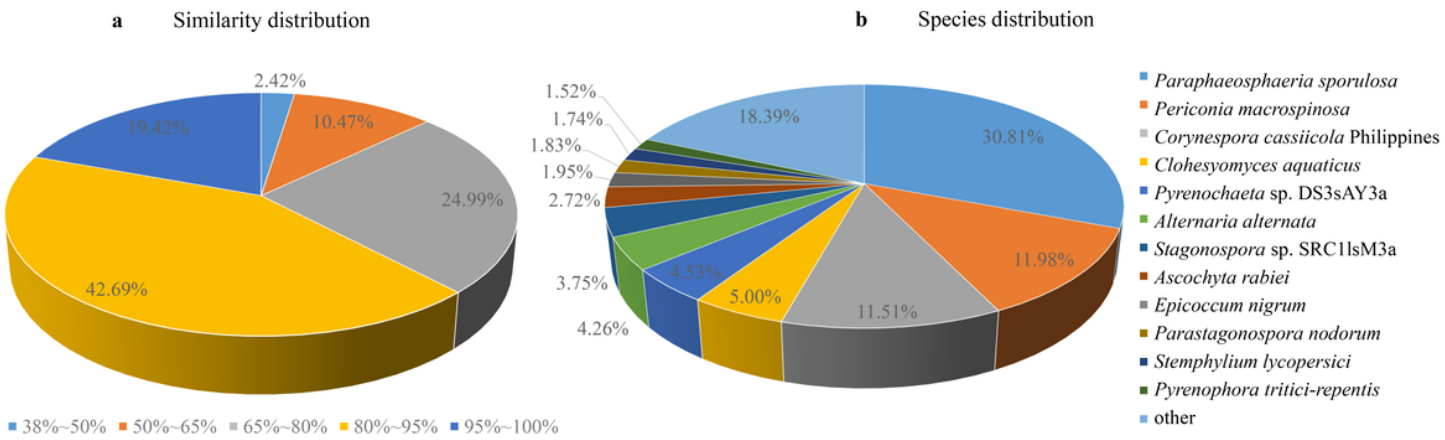

Figure 1

Non-redundant (Nr) classification analysis of the encoded proteins in the genome of C. minitans ZS-1. (a) and (b) represent the similarity distribution and species distribution of the Nr annotation based on the blast hit number, respectively.

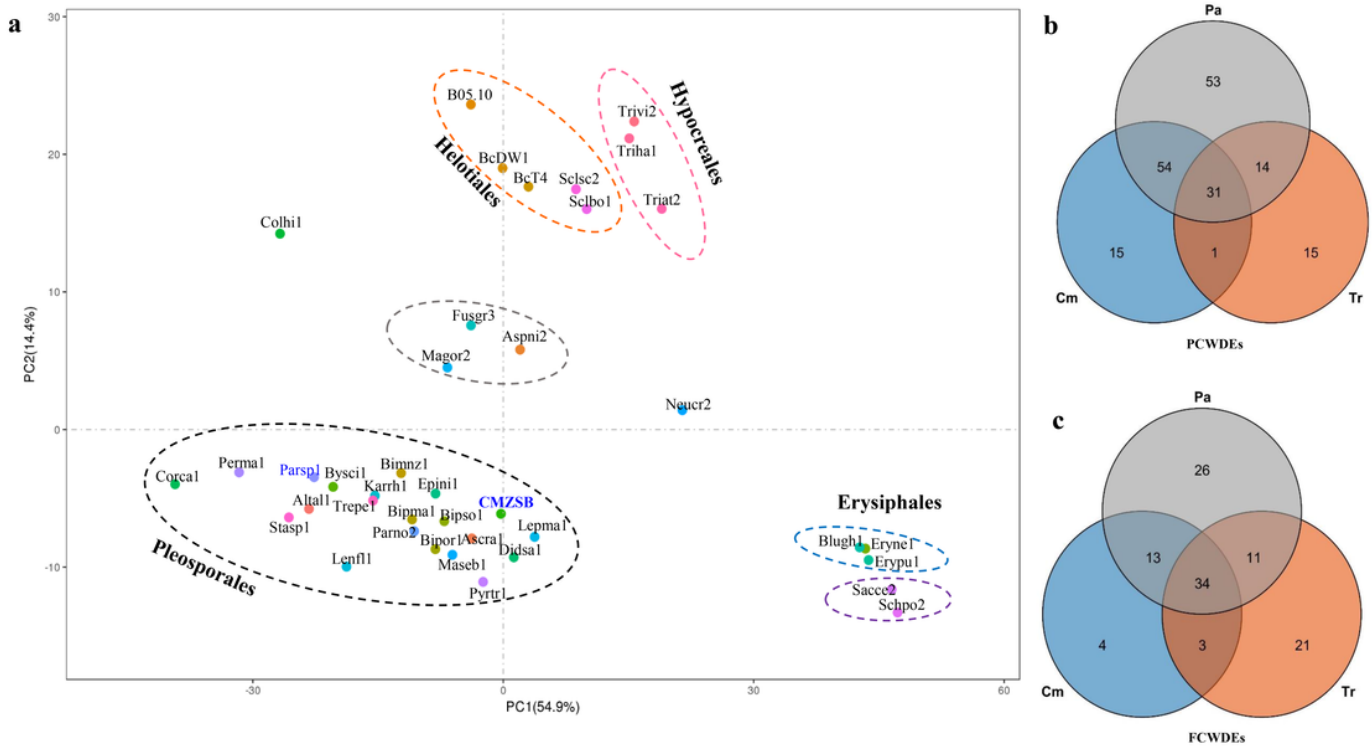

Figure 2

Comparison of CAZymes encoded in C. minitans ZS-1 and other 38 ascomycetes. (a) Multivariate grouping of ascomycete fungal genomes based on the protein number profiles of predicted CAZyme families using PCA. The CAZyme proteins from the fungal genomes were identified against the CAZy

database. A list of all proteins in each genome is shown in Additional file 1: Table S3. (b) Orthologous analysis of PCWDE-related protein comparison of C. minitans (Cm) with Trichoderma spp. (Tr) and 7 plant pathogens (Pa); C, PCWDE-related protein comparison of Cm with Tr and Pa. Orthologous groups were determined among the CAZymes encoded in the genomes of C. minitans, 3 Trichoderma spp. (T. atroviride, T. harzianum, T. virens) and 7 plant pathogens (S. sclerotiorum 1980, S. borealis, B. cinerea DW1, B. cinerea B05.10, B. cinerea BcT4, Parastagonospora nodorum SN15 and Pyrenophora tritici-repentis Pt-1C-BFP). P(F)CWDEs, plant (fungus) cell wall-degrading enzymes. Cm, CAZyme orthologous groups related to cell wall in C. minitans; Tr, CAZyme groups related to cell wall encoded in Trichoderma spp.; Pa, CAZyme orthologous groups encoded by the 7 plant pathogen genomes.

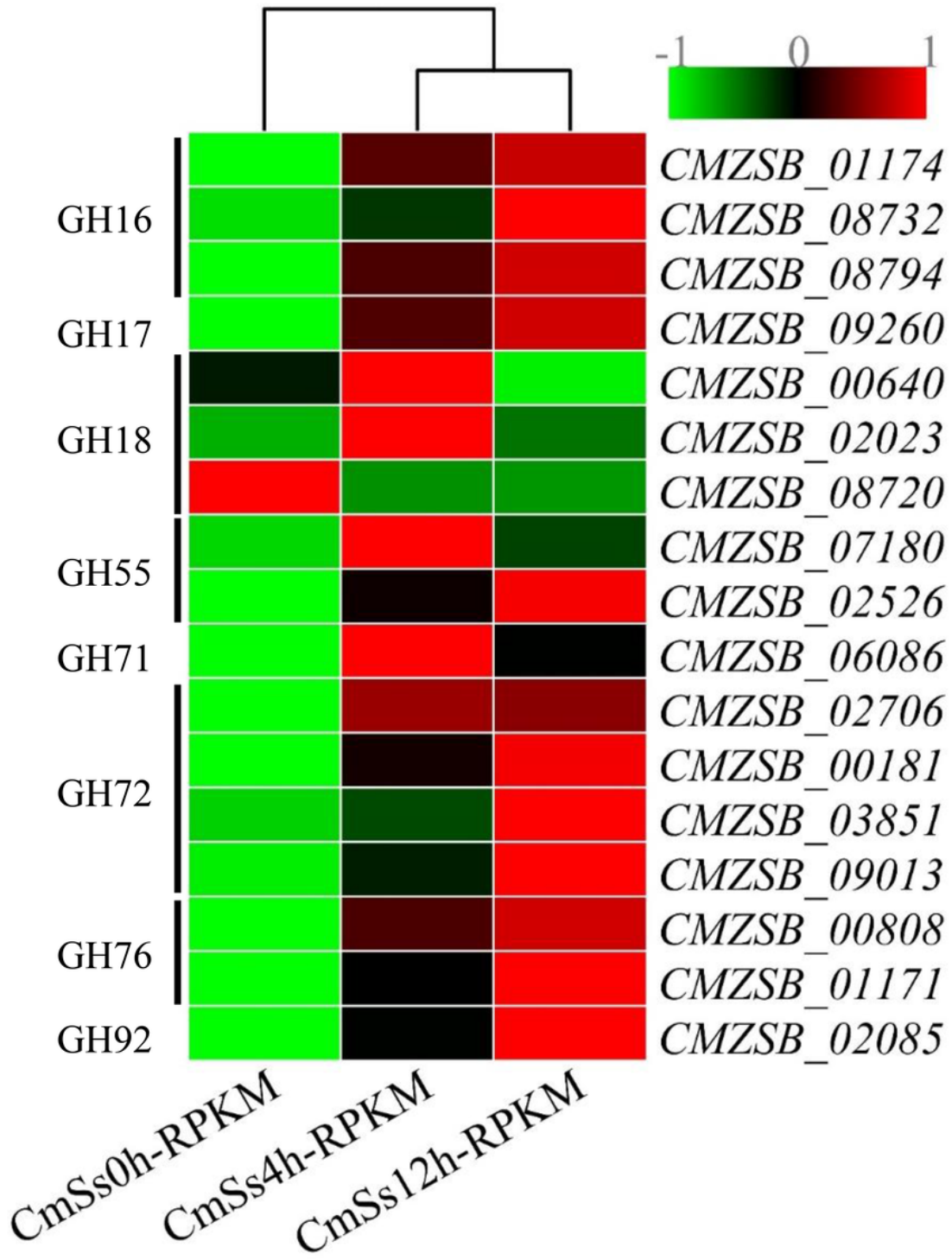

Figure 3

Expression of FCWDEs in the CAZymes detected during mycoparasitism. RPKM values at 3 interaction time points of 0 h, 4 h and 12 h

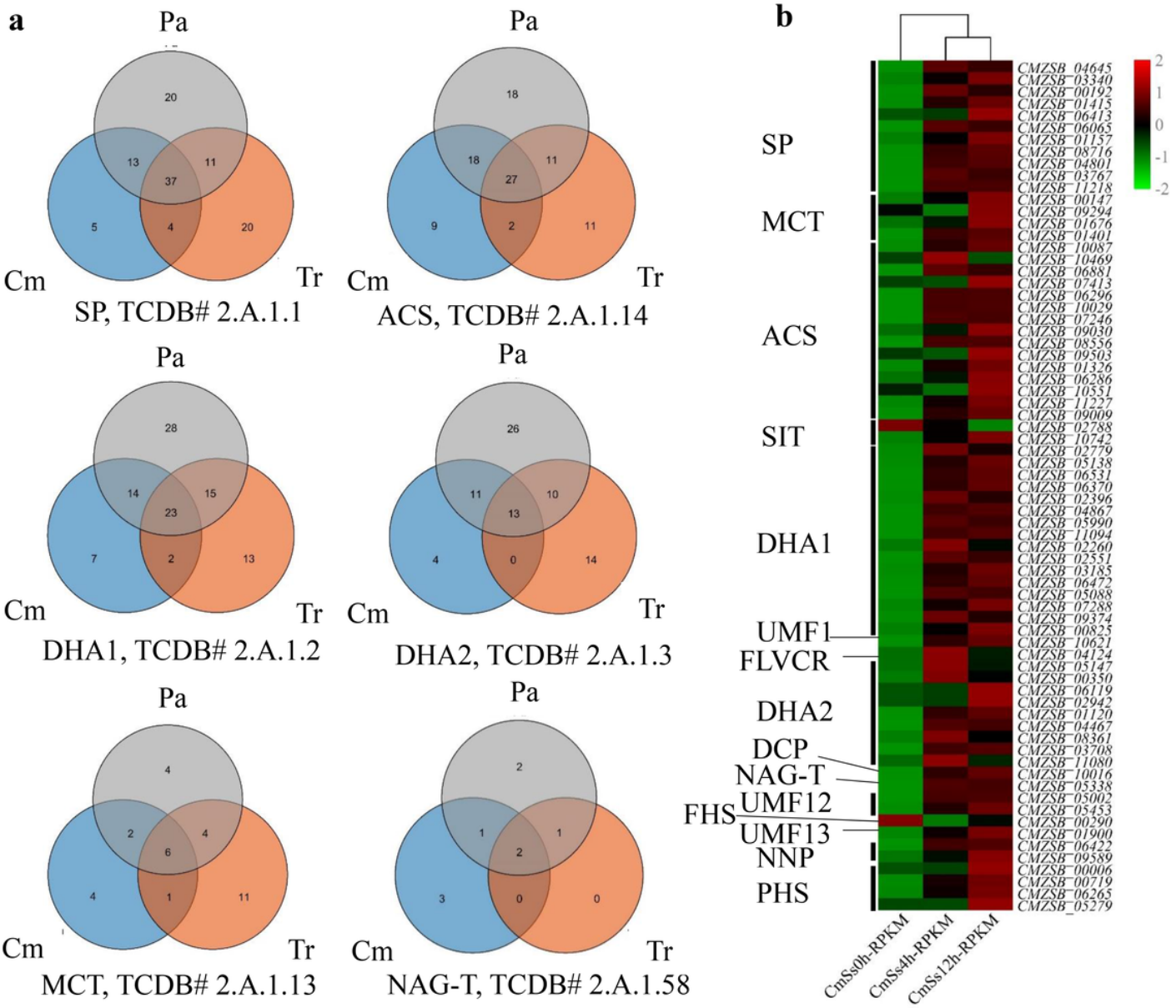

Figure 4

Distribution of the major facilitator superfamily transporters in the C. minitans ZS-1 genome and the DEGs involved in mycoparasitism. (a) Orthologous proteins groups distribution of SP, ACS, DHA1, DHA2, MCT and NAG-T in MFS transporters in 3 groups of Cm, Tr and Pa. (B) Gene expression of MFS transporters which detected significantly changed during the mycoparasitism stages of 0 h, 4 h and 12 h, respectively, in C. minitans. SP: Sugar Porter Family, ACS: Anion:Cation Symporter Family, DHA1: Drug:H+ Antiporter-1 (12 Spanner) Family, DHA2: Drug:H+ Antiporter-2 (14 Spanner) Family, MCT: Monocarboxylate Transporter Family, NAG-T: N-Acetylglucosamine Transporter Family, FHS: Fucose: H+ Symporter Family, PHS: Phosphate: H+ Symporter Family, OCT, Organic Cation Transporter Family, V-BAAT, Vacuolar Basic Amino Acid Transporter Family, SIT: Siderophore-Iron Transporter Family, LplT: Lysophospholipid Transporter Family, NNP: Nitrate/Nitrite Porter family, UMF1: Unidentified Major Facilitator-1 Family, LAT3: L-Amino Acid Transporter-3 Family, UMF12: Unidentified Major Facilitator-12

Family, UMF23: Unidentified Major Facilitator-23 Family, MHS: Metabolite:H+ Symporter Family, SHS: Sialate:H+ Symporter Family, FLVCR: Feline Leukemia Virus Subgroup C Receptor/Heme Importer Family, DCP: Major Facilitator Superfamily Domain-containing Protein 5 Family, Pl-Cu-UP: Plant Copper Uptake Porter, UMF30: Unidentified Major Facilitator-30 Family, YnfM: Acriflavin-sensitivity Family, PAT: Peptide/Acetyl-Coenzyme A/Drug Transporter Family, OFA: Oxalate:Formate Antiporter Family, ACDE: Aromatic Compound/Drug Exporter Family, PCFT/HCP: Proton Coupled Folate Transporter/Heme Carrier Protein Family, Pht: Proteobacterial Intraphagosomal Amino Acid Transporter Family. Sclsc2, S. sclerotiorum 1980; Sclbo1, S. borealis; BcDW1, B. cinerea DW1; B05.10, B. cinerea B05.10; Parno2, Parastagonospora nodorum SN15; Pyrtr1, Pyrenophora tritici-repentis Pt-1C-BFP; Triat2, Trichoderma atroviride; Triha1, Trichoderma harzianum; Trivi2, Trichoderma virens; CMZSB, C. minitans ZS-1 (this research); Parsp1, Paraphaeosphaeria sporulosa. Cm, orthologous groups of MFS transporters in C. minitans; Tr, orthologous groups of MFS transporters in Trichoderma spp.; and Pa, orthologous groups of MFS transporters in plant pathogens.

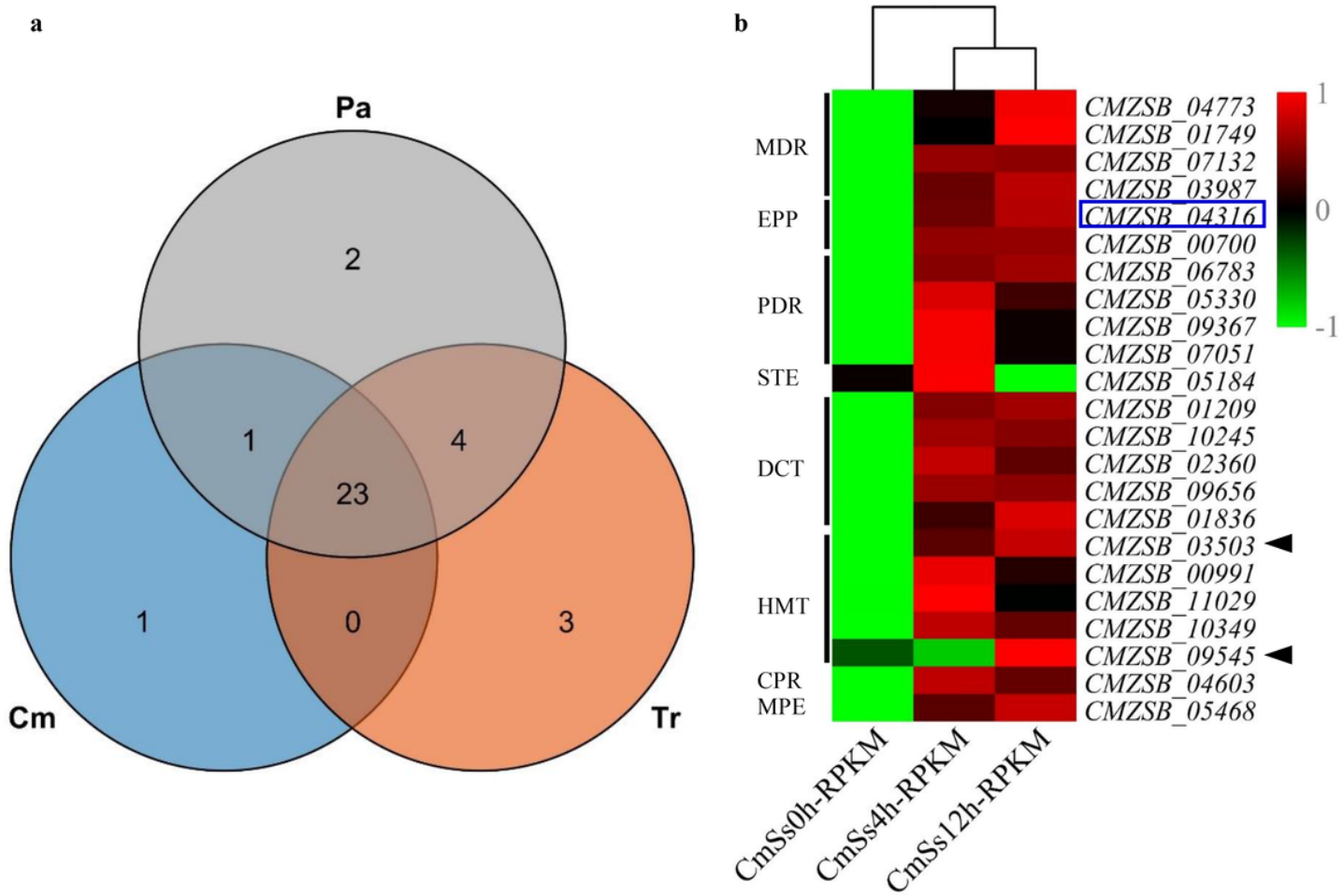

Figure 5

Orthologous proteins analysis of ABC family transporters in C. minitans ZS-1 and related fungal genomes. (a) Analysis of orthologous groups of ABC transporters in C. minitans, Trichoderma spp. and pathogen fungi. (b) Detected DEGs of transporters during the early stages of mycoparasitism. PDR:

Pleiotropic drug resistance, EPP: Eye pigment precursor transporter, Gld: Gliding motility ABC transporter, CPR: Cholesterol/phospholipid/retinal flippase, TauT: Taurine Uptake Transporter, U-ABC1: Unknown-ABC1, DrugE1: Drug exporter-1, BIT: Brachyspira Iron Transporter, B12-P: Cobalamine Precursor, PepT: Peptide/Opine/Nickel Uptake Transporter, PAAT: Polar Amino Acid Uptake Transporter, EVE: Ethyl Viologen Exporter, STE: a-Factor sex pheromone exporter, MPE: Mitochondrial peptide exporter, P-FAT: Peroxysomal fatty acyl CoA transporter, HMT: Heavy metal transporter, DCT: Drug conjugate transporter, MDR: Multidrug resistance exporter, DrugRA1: Drug resistance ATPase-1, DrugRA2: Drug resistance ATPase-2. The species-specific proteins encoding genes expression in C. minitans was represented of the black triangle; the blue box represented the gene of ABC transporters of the shared orthologous groups of C. minitans with Trichoderma spp..

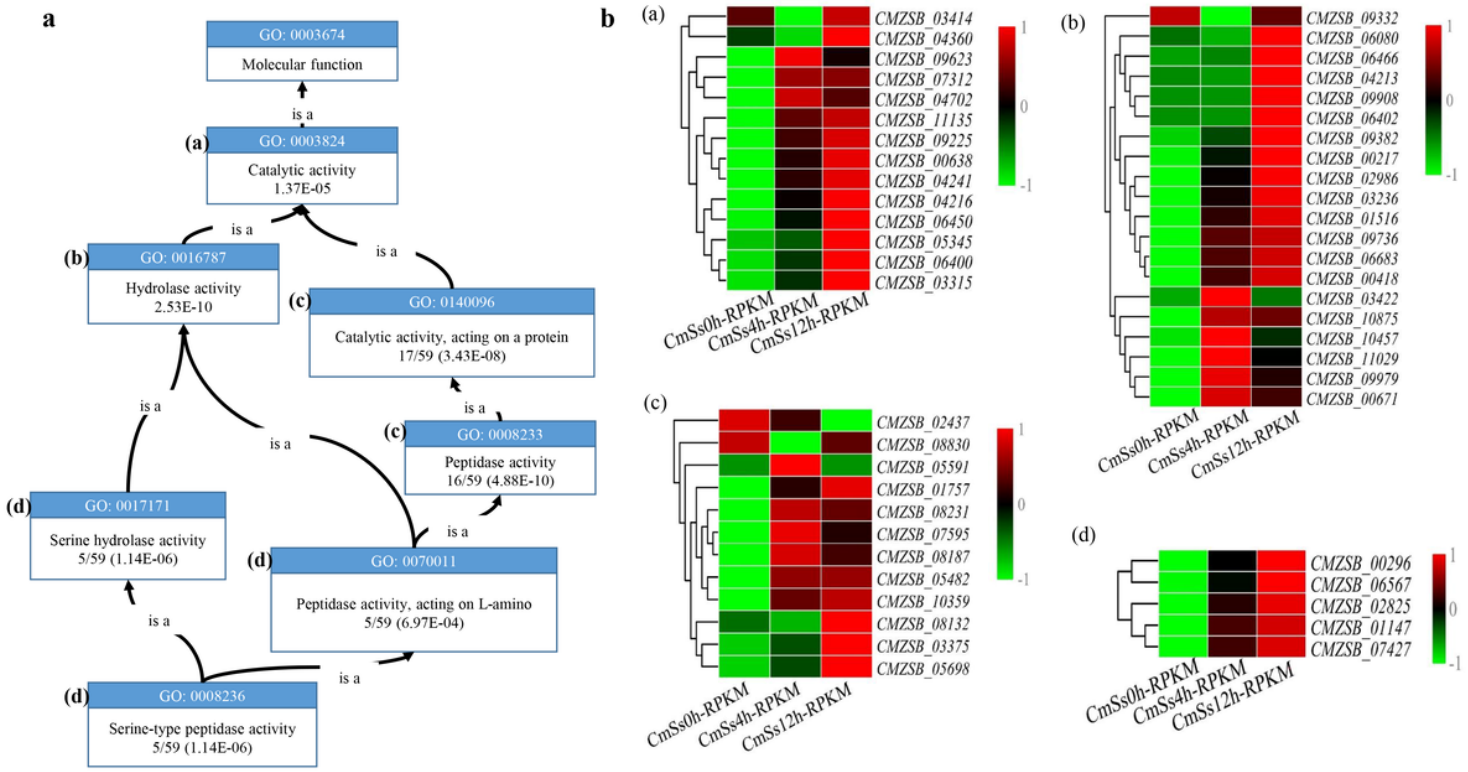

Figure 6

Serine peptidase secreted proteins in the mycoparasitism process in C. minitans. a, Enriched GO terms graph of serine peptidase of expressed secreted proteins. b, Expression of the DEGs related to mycoparasitism process of early stages: (a) Unique DEGs involved in GO: 0003824; (b) Unique DEGs involved in hydrolase activity in GO molecular function; (c) Unique DEGs related to GO: 0140096 and GO: 0008233, with CMZSB_08830 in GO: 0140096; (d) 5 DEGs related to each of GO: 0017171, GO: 0070011 and GO: 0008236. The graph of GO terms was downloaded and modified from https://www.ebi.ac.uk/QuickGO.

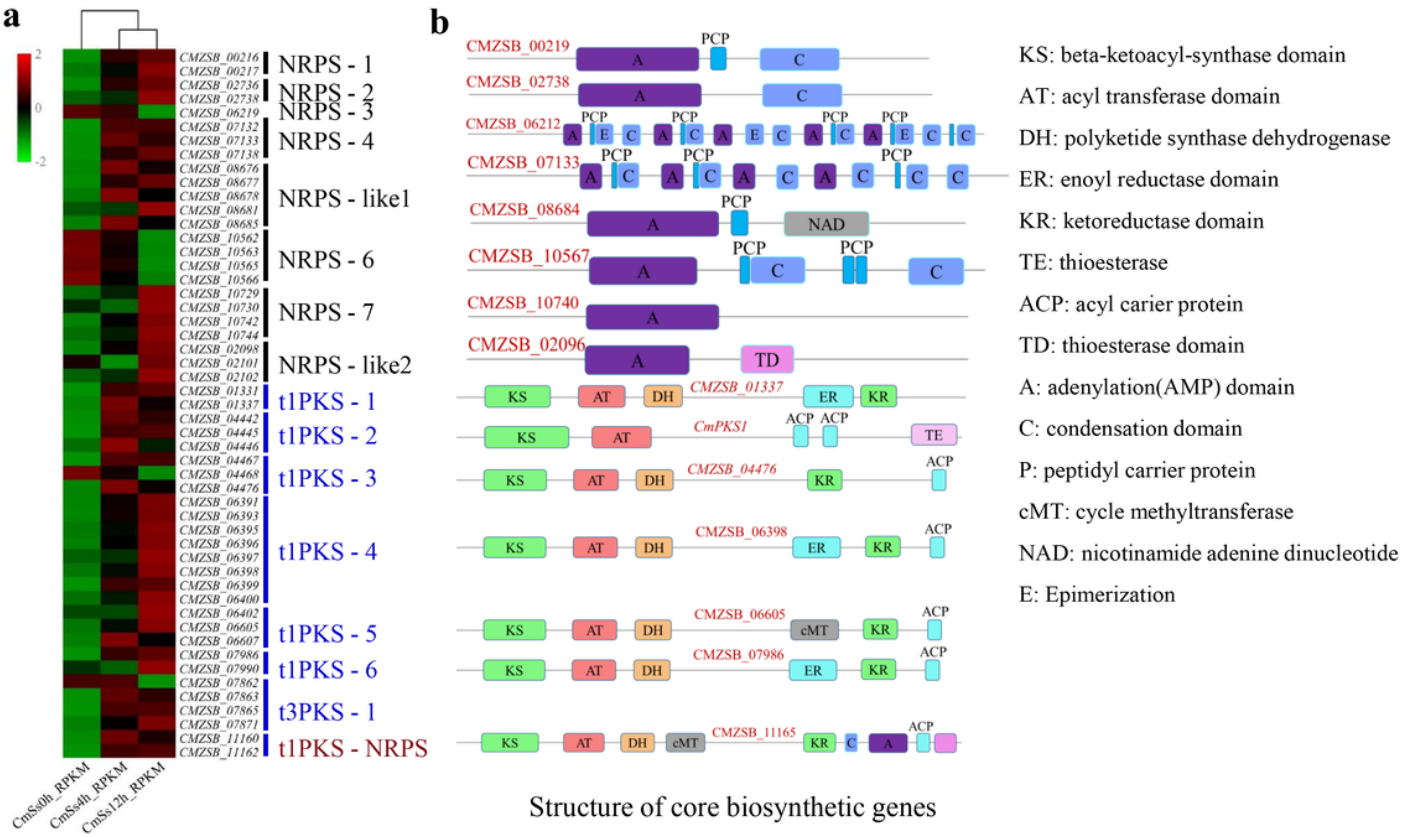

Figure 7

Gene expression and core biosynthetic genes related to secondary metabolism in C. minitans during the early stages of mycoparasitism. (a) Heatmap created with MeV (version 4.9.0) based on the RPKM values of the detected genes in C. minitans ZS-1; the RPKM values were normalized within the row for each gene; (b) Structures of core biosynthetic genes predicted to be involved in mycoparasitism in C. minitans ZS-1.

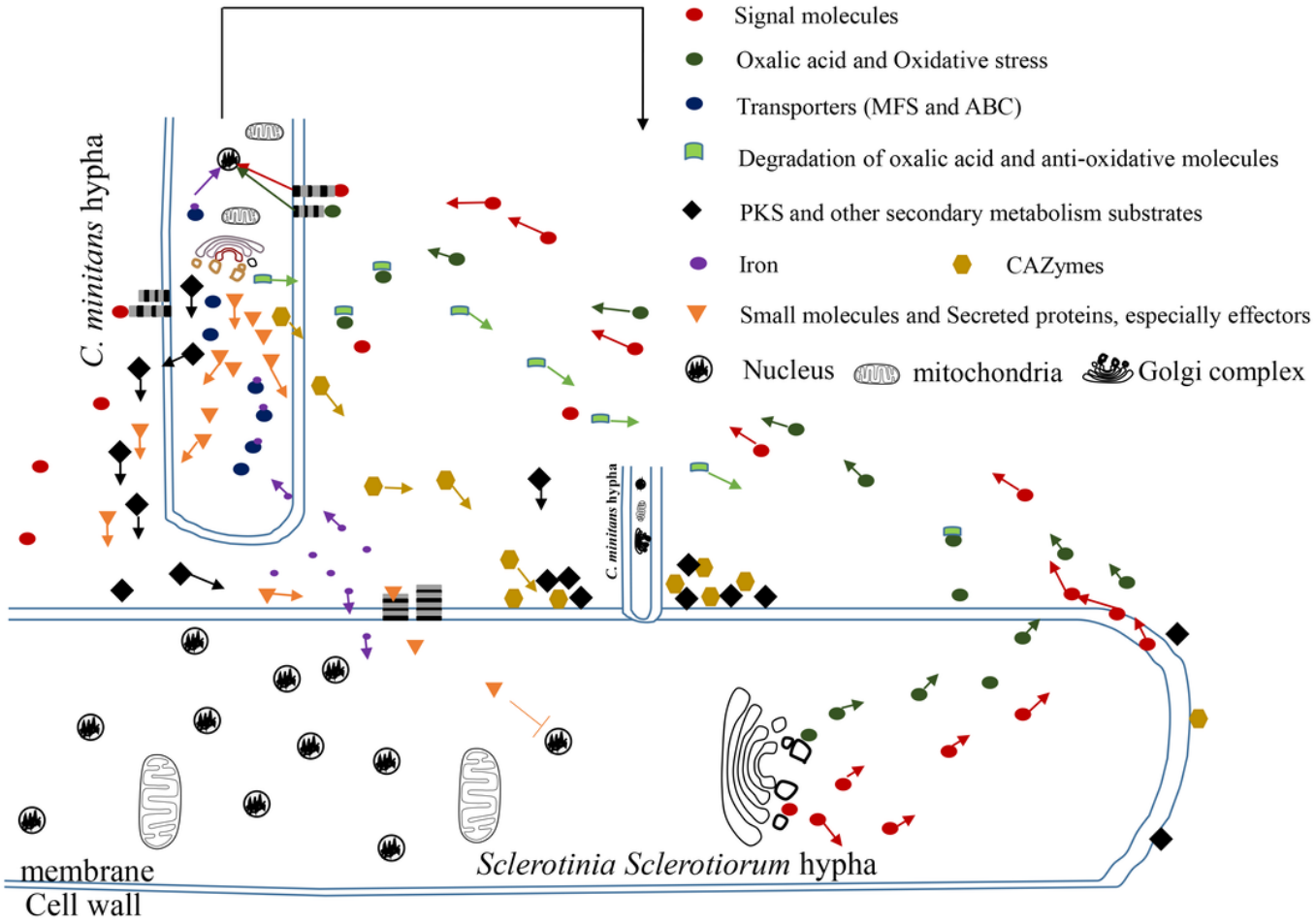

Figure 8

A predicted model of the mycoparasitism of C. minitans on its host fungus, S. sclerotiorum, as determined in this study.

Supplementary Files

This is a list of supplementary files associated with this preprint. Click to download.

- Additionalfile6.tif
- Additionalfile1.xls
- Additionalfile3.xls
- Additionalfile2.tif
- Additionalfile5.xls
- Additionalfile4.xls

- Additionalfile8.xls
- Additionalfile7.xls